The NF-κB family member RelB attenuates cigarette smoke-induced apoptosis in lung fibroblasts via transcriptional regulation of the aryl hydrocarbon receptor (AhR)

Matthew Iu

Department of Medicine
Division of Experimental Medicine, Meakins-Christie Laboratories
McGill University, Montreal
December 2015

A Thesis Submitted to McGill University in Partial Fulfillment of the Requirements of the Degree of Master of Science

Acknowledgements

I would like to extend my deepest gratitude to my supervisor, Dr. Carolyn Baglole, for her guidance and encouragement. Her continued belief in my abilities fuelled my own confidence to pursue challenging, yet exciting, research projects. To the members of the Baglole lab (Angela Rico de Souza, Michela Zago, Miles Sarill, and Necola Guerrina): I could not have asked for a better environment to cultivate my learning. The personalities of these individuals, which encapsulate dedication, hard work, and yet, joviality and kindness, were more than I could have hoped for. I would also like to acknowledge the faculty members of the Meakins-Christie Laboratories, particularly Dr. David Eidelman and Dr. Qutayba Hamid, for their consummate scientific advice. Finally, I must thank my family and friends: the completion of this chapter of my life would not have been possible without their uncompromising love and support.

TABLE OF CONTENTS

LIST OF ABBREVIATIONS

Abbreviation	*Meaning*
COPD	Chronic Obstructive Pulmonary Disease
NF-κB	Nuclear Factor Kappa B
AhR	Aryl Hydrocarbon Receptor
GOLD	Global Initiative for Chronic Obstructive Lung Disease
FEV1	Forced Expiratory Volume in 1 second
FVC	Forced Vital Capacity
α1AT	alpha 1-anti-trypsin
NE	Neutrophil Elastase
Bcl-2	B-cell lymphoma 2
OMM	outer mitochondrial membrane
IP	Immunoprecipitation
CS	Cigarette smoke
CSE	Cigarette smoke extract
MGMT	O6 methylguannine DNA methyltransferases
BER	base excision repair
NER	nucleotide excision repair
ROS	reactive oxygen species
RNS	reactive nitrogen species
IL	interleukin
SOD	superoxide dismutase
PAH	polycyclic aromatic hydrocarbon
B[a]P	Benzo [a] Pyrene
Cyp1a1/b1	cytochrome P450 enyzymes
Nqo1	NADPH dehydrogenase quinone 1
ECM	extracellular matrix
ActD	actinomycin D
Cox	cyclooxygenase
CD	cluster of differentiation
RHD	rel homology domain
DBD	DNA binding domain
NLS	nuclear localization sequence
siRNA	short interfering ribonucleic acid
MLF	mouse lung fibroblast

ABSTRACT

Chronic Obstructive Pulmonary Disease (COPD) is a chronic and prevalent respiratory disease caused primarily by long term inhalation of cigarette smoke. A major hallmark of COPD is elevated apoptosis of structural lung cells including fibroblasts. The NF-κB member RelB may suppress apoptosis in response to cigarette smoke, however its function in lung cell survival is not known. RelB may act as a pro-survival factor by controlling the expression of anti-oxidants such as superoxide dismutase 2 (Sod2). Sod2 is also controlled by the aryl hydrocarbon receptor (AhR), a ligand-activated transcription factor known to suppress cigarette smoke-induced apoptosis. As the AhR is also a binding partner for RelB, we speculate that RelB suppresses cigarette smoke-induced apoptosis by regulating the AhR. Using an *in vitro* model of cigarette smoke exposure (cigarette smoke extract [CSE]), we found that CSE down-regulated RelB expression in mouse lung fibroblasts, which was associated with elevated levels of the apoptosis marker cleaved PARP. Genetic ablation of RelB elevated CSE-induced apoptosis. $RelB^{-/-}$ cells also displayed significantly decreased AhR mRNA and protein expression, concomitant with loss of AhR target gene expression (Cyp1a1, Cyp1b1, Nqo1, and Sod2). Finally, we identified 4 putative RelB binding sites in the AhR gene, and via chromatin immunoprecipitation assay, demonstrated that RelB binds at 3 of these sites. Overall, these data support that RelB suppresses cigarette smoke-induced apoptosis by regulating the AhR, potentially by binding to its gene and affecting transcription. Together, these two proteins may comprise an important cell survival signalling pathway that reduces apoptosis upon cigarette smoke exposure.

RÉSUMÉ

La maladie pulmonaire obstructive chronique (MPOC) est une maladie respiratoire

chronique et répandue et est causée principalement par l'inhalation de fumée de cigarette à long terme. Une caractéristique importante de la MPOC est un niveau élevé d'apoptose des cellules pulmonaires structurelles, notamment de fibroblastes. RelB, un membre de la famille NF-kB, peut supprimer l'apoptose en réponse à la fumée de cigarette mais toutefois, sa fonction dans la survie des cellules pulmonaires n'est pas encore connue. RelB peut agir comme un facteur pro-survie en contrôlant l'expression d'antioxydants tels que la superoxyde dismutase 2 (Sod2). Sod2 est également contrôlée par le récepteur d'hydrocarbure d'aryle (AhR), un facteur de transcription activé par un ligand qui inhibe l'apoptose induite par la fumée de cigarette. Comme l'AhR est également un partenaire de liaison pour RelB, nous spéculons que RelB réprime l'apoptose induite par la fumée de cigarette en régulant l'AhR. En utilisant un modèle *in vitro* d''exposition à la fumée de cigarette (extrait de fumée de cigarette [CST]), nous avons trouvé que la CST à diminué l'expression de RelB dans les fibroblastes de poumon de souris, ce qui a été associé avec des niveaux élevés de PARP clivé. L'ablation génétique de RelB a augmenté l'apoptose induite par le CST. Les cellules RelB $^{-/-}$ affichent également une diminution significative d'ARNm et de protéine AhR, concomitante avec la perte de l'expression de ses gènes cibles (Cyp1a1, Cyp1b1, Nqo1, et Sod2). Finalement, nous avons identifié 4 sites de liaison putatifs pour RelB dans le gène AhR, et via un essai d'immunoprécipitation de chromatine, nous avons démontré que RelB se lie à 3 de ces sites. Dans l'ensemble, ces données confirment que RelB supprime l'apoptose induite par la fumée de cigarette en régulant AhR, potentiellement en se liant à son gène et en affectant sa transcription. Nous pensons qu'ensemble, ces deux protéines font partie d'une importante voix de signalisation de survie cellulaire réduisant l'apoptose suite à une exposition à la fumée de cigarette.

CHAPTER 1: INTRODUCTION

1.1 COPD: disease characteristics, healthcare burden

Cigarette smoking remains the leading cause of preventable death worldwide, contributing to the pathogenesis of several diseases such as lung cancer, cardiovascular disease, and chronic obstructive pulmonary disease (COPD) (1). COPD is a complex respiratory disease defined by poorly reversible airflow limitation and manifesting as chronic bronchitis and/or emphysema (2). The death rates of other major diseases in the US, such as cardiovascular disease, have decreased over recent years whereas COPD mortality rates have continued to rise (3). One of the major sources of mortality from COPD is exacerbations (4), which are characterized as episodes of severe respiratory symptoms including elevated dyspnea and coughing, frequently requiring hospitalization (4). From a healthcare perspective, exacerbations are costly, as they dramatically increase hospital stays; one study had determined that the median cost following an exacerbation for a single patient was $7,100 (5). Global economic costs for COPD, though challenging to calculate, have been estimated at approximately $24 billion per year in the US alone (6). Another component of COPD that contributes heavily to mortality is the existence of co-morbidities, which include cardiovascular disease, cancer, cachexia, diabetes, and depression (7). Together, both exacerbations and co-morbidities galvanize the need for robust clinical characterization of COPD.

1.1.1 COPD: clinical diagnosis, pathological features, treatment options

The primary clinical tool utilized to diagnose COPD is spirometry. Patients are evaluated by the ratio of their FEV_1 (forced expiratory volume in 1 second) to FVC (forced vital capacity); this measurement can be conceptualized as the fraction of the maximum volume of air that can

be exhaled in 1 second (3). Typically, COPD is confirmed if the FEV_1/FVC ratio is < 0.7 and the FEV_1 is < 80% of predicted (3). According to the Global Initiative for Chronic Obstructive Lung Disease (GOLD) staging (8), patients are codified between GOLD 0-IV in increasing order of severity based on their FEV_1 and FVC measurements (**Table 1**).

Table 1. Global Initiative for Chronic Obstructive Lung Disease (GOLD) staging. Patients are scored based on spirometry parameters, FEV_1 and FVC, in addition to clinical symptoms such as cough, sputum, and dyspnea.

Stage	FEV1/FVC	FEV1 % predicted	Symptoms
0 (at risk)	>0.7	>80%	Cough, sputum
I (mild)	<0.7	>80%	Cough, sputum
II (moderate)	<0.7	<80%	Cough, dyspnea
III (severe)	<0.7	<50%	Cough, dyspnea
IV (very severe)	<0.7	<30%	Respiratory failure

From a pathology perspective, COPD possesses numerous characteristic features (9). These include extracellular matrix degradation, inefficient tissue repair, compromised angiogenesis, and chronic inflammation (9). The major inflammatory cell types in COPD are macrophages and neutrophils (10). It is postulated that cigarette smoke aberrantly activates macrophages, leading to their recruitment to the lungs (numbers can be increased 5 -10 fold in the bronchoalveolar lavage of COPD subjects); these cells, in turn, release neutrophil chemotactic factors and thereby drive the inflammatory phenotype of this disease (10). Concomitant with the chronicity of inflammatory cell recruitment in the lung are also increases in cytokines such as tumour necrosis factor-α (TNF-α) and matrix metalloproteases (MMPs);

heightened TNF-α can promote the activation of the nuclear factor kappa B family (NF-κB), which produces IL-8, a potent neutrophil chemoattractant (10).

Unfortunately, there are limited therapeutic options for patients afflicted by this disease. The primary treatment for COPD patients is bronchodilators, comprised of β2-agonists and anti-cholingerics. The former group operates with an incompletely understood mechanism of action but has been shown to increase skeletal muscle mass and improve patient symptoms; the latter group relies on the inhibition of muscarinic receptors, which when antagonized relieve mechanical forces in the lung (7). A second treatment option for COPD is corticosteroids, aimed at curtailing the inflammatory component of COPD. These are designed to activate the glucocorticoid receptor (GR) to decrease pro-inflammatory gene expression (11). Unfortunately, COPD patients commonly develop insensitivity to corticosteroids (11). Apart from drug-based therapies, pulmonary rehabilitation utilizing exercise regimens is another strategy employed to moderate the symptoms of COPD, and is particularly useful for relieving the anxiety and depression components of the disease (7). However, even with these treatment options in place, there is still suboptimal long-term improvement in patients. Therefore, there is an increasing rationale to develop new therapies aimed at COPD treatment and management. This necessitates research into the cellular and molecular mechanisms governing the progression from smoke inhalation to COPD development.

1.1.2 Emphysema: characteristics and features

Emphysema is a component of COPD defined by extensive destruction to the lung parenchyma, leading to airspace enlargement distal to the terminal bronchioles (13). The functional consequences include affecting the recoil of the lungs and therefore the propensity for

gas exchange. Compliance of the lung (defined as the change in lung volume for a given pressure) is dramatically increased, which interferes with efficient breathing (14). Furthermore, airway narrowing due to chronic inflammation promotes increased resistance, thus requiring greater work of breathing (15).

How chronic smoking leads to alveolar destruction is not fully understood and likely involves multiple dysregulated biological processes. One of these mechanisms is immune cell recruitment and their excessive release of proteases, particularly neutrophil elastase (NE) (16). Excessive activity of proteases such as NE leads to destruction of the alveolar architecture. Experimental evidence for this comes from animal models of emphysema whereby NE-deficient ($NE^{-/-}$) mice exposed to chronic cigarette smoking regimens were significantly protected from developing airspace enlargement, a feature indicative of emphysema (16). In individuals with genetic deficiency of alpha 1 anti-tyrpsin (α1-AT), which inhibits NE, homozygous recessive individuals who smoke possess a significantly higher probability of developing emphysema (17). Another mechanism postulated in the development of emphysema is dysregulated apoptotic death of structural cells in the lung, including epithelial cells and fibroblasts (18). In this way, it is speculated that excessive apoptosis compromises the lung architecture, thereby contributing to emphysematous destruction (18).

1.2 Apoptosis

Apoptosis is an energy-requiring process of regulated cell death, which is essential for maintaining homeostasis in multi-cellular organisms (19). Apoptosis is utilized during embryonic development to eliminate unneeded cells for correct foetal development of organs such as the lung (20). Apoptosis is also utilized for maintaining adult tissue homeostasis, where

gut epithelial cell apoptosis is employed as a turnover mechanism (21). Moreover, apoptosis is also an effective strategy for eliminating compromised cells (22). Cells infected with viruses pose a global threat to the host and thus, apoptosis is one of the defences utilized in immune responses (22). Apoptosis of alveolar macrophages, for example, is an innate immune response against *Mycobacterium tuberculosis* to contain the spread of the pathogen (23). Another trigger of apoptosis is excessive DNA damage, which promotes a risk of tumourigenesis. In response to moderate DNA damage, cells orchestrate a variety of DNA repair processes in an attempt to preserve viability, including activation of O6 methylguannine DNA methyltransferases (MGMT), base excision repair (BER), and nucleotide excision repair (NER) enzymes (28). However, once the cell has accrued severe DNA damage, particularly in the form of double stranded breaks, it commits to apoptosis to limit potential risk towards the organism (28). Thus, apoptosis is one mechanism employed to eliminate potential cancerous cells (24). The tumour suppressor p53 eliminates cancer cells in part, through activation of the apoptotic pathway (25). Conversely, one of the major hallmarks of many types of tumours is insensitivity to apoptosis, which provides cancer cells with a useful adaptation for both initiating and perpetuating abnormal growth (26). Many chemotherapeutic strategies are aimed at inducing apoptosis in tumours (27). It is tempting to envision apoptosis as a wholly beneficial process to the host. However, excessive apoptosis can also lead to cell and tissue destruction and promote diseases such as emphysema (29).

At the cellular level, apoptosis is identified by morphological changes, including membrane blebbing and chromatin condensation; these events culminate in the formation of apoptotic bodies which are then are removed from the local milieu in order to prevent excessive inflammation (30). This removal is accomplished by “professional phagocytes” including

dentritic cells (DCs) and macrophages that recognize molecular signatures on the surfaces of the apoptotic bodies such as phosphatidylserine (PS), to signal engulfing (36). Mechanistically, apoptosis is achieved through two pathways: the intrinsic and the extrinsic pathways (31). In the intrinsic pathway, intracellular stresses such as excessive DNA damage promote the up-regulation of pro-apoptotic factors (*e.g.* Bax) associated with the outer mitochondrial membrane (OMM) (32). Typically Bax is titrated by the inhibitory action of pro-survival factors such as B cell lymphoma 2 (Bcl-2) (32). When the Bax:Bcl-2 ratio is increased, this promotes the opening of mitochondrial pores that allow soluble factors, such as cytochrome-c, to permeate into the cytosol (32), leading to the activation of the Apaf-1 complex, an ATP-consuming machinery that allows for the initiation of caspases (31). Caspases are the effector proteins for apoptosis, but are typically found in inactive conformations (33). Upon initiation of apoptosis, caspases are processed into smaller and active forms that in turn cleave cellular macromolecules, such as lamin, causing the morphological features of apoptosis (33). In the extrinsic pathway, activation of "death receptors" including Fas-associated Protein with Death Domain (FADD) by ligands such as FasL lead to the activation and cleavage of caspase-8 (34). Both intrinsic and extrinsic pathways culminate with the cleavage of caspase-3, the ultimate effector of apoptosis (35).

1.2.1 Oxidative Stress: a trigger for apoptosis

One of the stimuli for apoptosis is reactive oxygen species (ROS) or reactive nitrogen species (RNS) that lead to "oxidative stress", a scenario in which these molecules exist in excess over the capacity of the antioxidant response (37). ROS/RNS contain an unstable unpaired electron, providing a greater propensity for chemical reactions with biological macromolecules that cause cellular damage and include lipid peroxidation, protein oxidation, and DNA damage

(37). At physiological levels ROS/RNS also possess signalling roles in homeostatic processes including cell survival (38). For instance, one group has recently found that longevity in *C. Elegans* is extended by ROS activation (38).

It is therefore only under persistently high doses of oxidants that these species become detrimental (39), as cells have evolved antioxidant machinery to combat ROS/RNS (40). The superoxide dismutase (Sod) family of enzymes and non-protein thiol glutathione (GSH) are among a host of factors that convert unstable oxidants into benign compounds (40). One of the fundamental antioxidant reactions is the Sod-dependent conversion of superoxides ($O_2^{\bullet-}+O_2^{\bullet-} \rightarrow H_2O_2+O_2$) followed by the GSH-dependent reduction of hydrogen peroxide to water and oxygen (40). This latter reaction is achieved by 2 GSH molecules undergoing reduction in their SH groups and forming a GS-SG bond; glutathione reductase then uses NADPH to reduce GSSG back to two molecules of GSH for repetition of the cycle (40). Biochemical mechanisms such as these are an integral component of maintaining cellular homeostasis. When ROS/RNS concentrations exceed the threshold of these antioxidant defences to function, the net result is oxidative stress and damage occurs to cellular macromolecules that may initiate apoptosis (39). Importantly, cigarette smoke is an abundant source of ROS/RNS and therefore may induce excessive apoptosis in lung cells (41).

1.2.2 Cigarette smoke and apoptosis induction

Cigarette smoke is a complex mixture containing over 4,000 compounds, including ROS/RNS (41-44). Chemical estimates suggest that a single puff of smoke contains in the order of $10^{15\text{-}17}$ oxidants (41-44), thereby imposing a high oxidative burden on the lungs. Moreover, apart from ROS/RNS-based damage, cigarette smoke itself contains compounds that can

intercalate DNA and activate the apoptotic pathway (45). In particular, the incomplete combustion of cigarettes promotes the formation of polycyclic aromatic hydrocarbons (PAH) such as Benzo[*a*]Pyrene (B[*a*]P) (45). PAHs activate members of the CYP1 family of enzymes. Chemical reactions mediated by CYPs convert these into bulky abducts (*e.g.* N^2-Benzo[a] Pyrene), which possess the capacity to diffuse into the nucleus and directly intercalate DNA; these substitutions represent a form of DNA damage and in excessive amounts, lead to apoptosis (45). In the context of the lung, exposure to these genotoxic and oxidative compounds found in cigarette smoke can initiate apoptosis in several cell types, including fibroblasts (18, 41-44).

1.3 Lung fibroblasts

The lung is a highly complex organ comprised of a heterogeneous population of cell types including epithelial and endothelial cells as well as fibroblasts (46). Lung fibroblasts are an important cell type for preserving the architecture of the parenchyma via their production of extracellular matrix (ECM), a heterogeneous mixture of proteins including collagen, proteoglycans, and elastins, which is essential for providing other lung cells with a scaffold for forming adhesions (47). In emphysema patients, there is significantly higher oxidative stress and apoptosis in multiple lung cell types, including epithelial and endothelial cells and fibroblasts (18). Interestingly, lung fibroblasts from emphysema subjects display slower proliferation (48) and increased senescence (49) *in vitro* when compared to smoker controls (without evidence of emphysema), suggesting that injury of these cells may be an important feature of this disease. Elevated apoptosis in lung fibroblasts, in particular, carries important consequences for other lung cell types (50). As fibroblasts are the major producers of ECM, their loss galvanizes a deficiency of this scaffold for other cells in the lung such as epithelium (50). This can further

perpetuate apoptosis as loss of cell attachment induces a particular form of cell death known as anoikis (50). Consequently, protection of lung fibroblasts against cigarette smoke-induced apoptosis may represent a useful strategy for the treatment and management of the emphysema component of COPD. In order to do so however, it is requisite to understand the molecular mechanisms regulating apoptosis in these cells upon cigarette smoke exposure.

1.4 The NF-κB Family

Although the molecular mechanisms that regulate oxidative stress and apoptosis upon cigarette smoke exposure are not well-defined, one group of proteins associated with apoptotic regulation belong to the NF-κB family. NF-κB proteins are a group of transcription factors highly conserved throughout eukaryotes and are ubiquitously-expressed in many organisms (51). The NF-κB family is comprised of five members: RelA (p65), RelB, c-Rel, NF-κB1 (p50) and NF-κB2 (p52) (51). All of these share a conserved RHD (Rel Homology Domain) (52) comprised of a DNA binding domain for activation of target genes, a dimerization domain for forming homo and heterodimers with other NF-κB members, and a NLS (nuclear localization sequence) for targeting to the nucleus. RelA, RelB, and c-Rel also contain a trans-activation domain requisite for gene binding. NF-κB1 and NF-κB2 lack this sequence because they are cleaved from the larger precursor proteins p105 and p100 respectively; p105 and p100 typically function as binding partners for RelA, RelB, and c-Rel (52). Genetic and biochemical analyses have revealed that these NF-κB members contain unique consensus binding sites, which contribute towards their specificity of action (53). Moreover, NF-κB members may achieve additional specificity by partnering with unique chromatin remodelling complexes, such as SWI/SNF in the case of RelB (54). The roles of NF-κB are diverse and include regulation of

immunity and cell survival (55). Two primary NF-κB pathways have been well-characterized: the canonical and the non-canonical (alternative) pathways (**Figure 1**) (56).

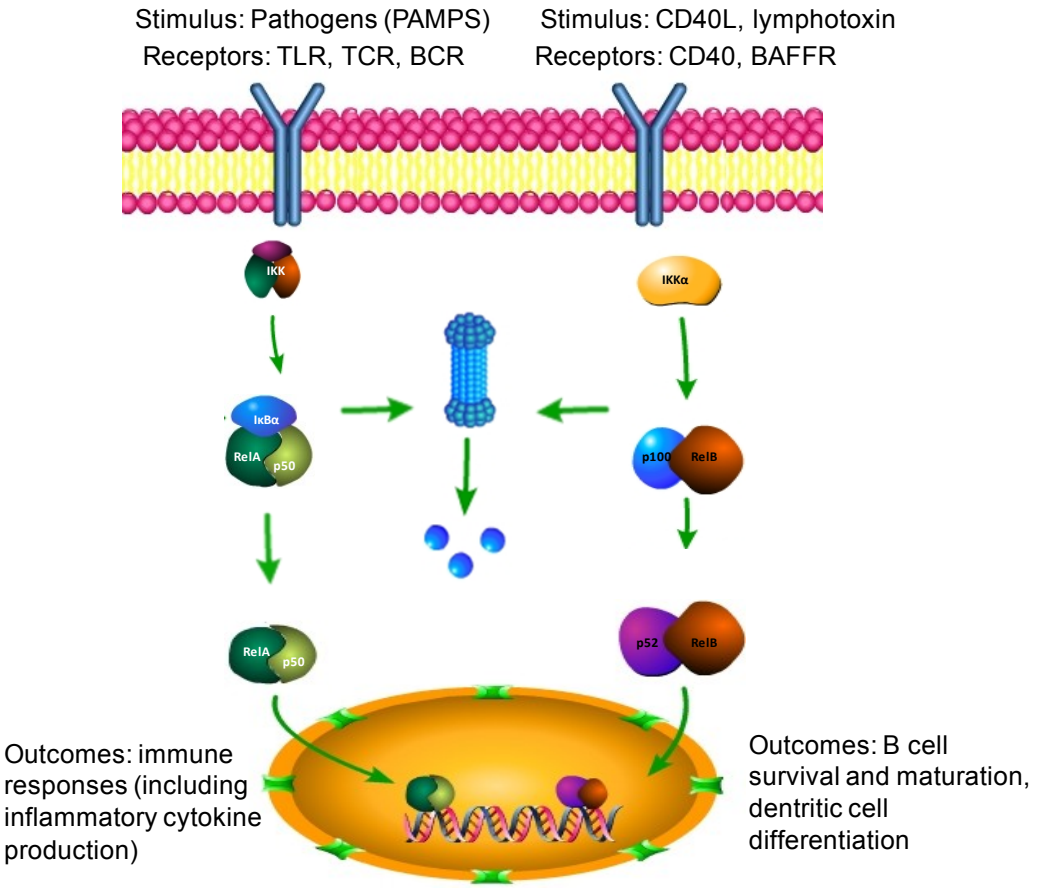

Figure 1. **Scheme of NF-κB Signalling.** NF-κB signals through the canonical and the non-canonical (alternative) pathways. In the canonical pathway (left) RelA and p50 are sequestered in the cytoplasm by IκBα, which is degraded by IKK-dependent phosphorylation upon stimulation of the pathway by receptors such as TLRs. In the non-canonical pathway (right) RelB and p100 are sequestered in the cytoplasm by the inhibitory region of p100's C-terminus, which is spliced to p52 following IKKα-dependent phosphorylation. This pathway is activated by receptors such as CD40.

1.4.1 The Canonical NF-κB Pathway

The canonical pathway has been the most extensively studied due to its role in immune responses and apoptosis suppression (57). In the canonical NF-κB pathway (**Figure 1**- left), p105 is constitutively processed into p50. RelA interacts with p50, which are sequestered together in the cytoplasm via the inhibitory protein IκBα. During an infection, for example, activation of toll-like receptors (TLR) results in phosphorylation of IκBα, leading to its degradation via the proteasome. This permits RelA and p50 heterodimers to translocate to the nucleus for subsequent activation of target genes (51). In addition to immunity, numerous studies indicate that RelA suppresses apoptosis in diseases such as cancer through the up-regulation of pro-survival genes such as IAP (inhibitors of apoptosis) family members as well as Bcl-2 (58).

1.4.2 The non-canonical (alternative) NF-κB pathway

The major functions of the non-canonical or alternative NF-κB pathway are in immune cell and organ development, such as lymphoid cell differentiation and maturation (51). In this pathway, RelB interacts with the precursor NF-κB protein p100, which possesses an IκBα-like inhibitory sequence for sequestering RelB in the cytoplasm. Upstream receptors for this NF-κB pathway include CD40 and Receptor Activator of Nuclear Factor κB (RANK), and whose activation leads to the phosphorylation and processing of p100 to p52; RelB and p52 then translocate to the nucleus and activates genes involved in processes such as lymphoid cell development (51). Apart from roles in lymphoid cell development, the non-canonical pathway also orchestrates immune resolution (59). Historically, RelB was identified as inhibitory-Rel (I-Rel), signifying its role in inhibiting the pro-inflammatory activity of canonical NF-κB (RelA) (59). In this manner, it has been found that RelB can function as an antagonist for RelA activity

by forming inactive heterodimers in response to inflammatory stimuli such as lipopolysaccharide (LPS) and thereby preventing RelA binding to target sequences (60). This anti-inflammatory phenotype is exemplified by the RelB-deficient mouse, which demonstrates multi-organ inflammation, including the spleen and lung (61). In particular to the lungs, these mice exhibit a progressive increase in inflammation over time, evident as early as 8-10 days old, with an increase in perivascular mononuclear cell infiltrate primarily comprised of lymphocytes; there are also granulocytes and excessive alveolar macrophages present in these lungs (61).

1.4.3 RelB: roles in suppressing cigarette smoke-induced inflammation

RelB is increasingly recognized for its role in regulating pulmonary inflammation in response to cigarette smoke. We and others have demonstrated that RelB suppresses the expression of cyclooxygenase-2 (COX-2), an inducible enzyme which produces immunoregulatory prostaglandins (PGs) such as PGE_2 (62,63). RelB over-expression in the lungs also attenuates cigarette smoke-induced neutrophilia and pulmonary COX-2 levels (64). Finally, we have recently shown that RelB levels are reduced in lung fibroblasts from smokers with and without COPD (65). Together, these studies highlight the importance of RelB against the deleterious effects of cigarette smoke. However, the role of RelB in regulating apoptosis in response to cigarette smoke is not known but may have important implications for the emphysema component of COPD.

1.4.4 RelB: roles in suppressing apoptosis

While the role of RelB in mediating apoptosis in the respiratory system is unknown, accumulating evidence supports that RelB suppresses apoptosis. In B cells, Mineva *et al*

demonstrated that RelB was required to rescue these cells from apoptosis in part by regulating the levels of the anti-oxidant protein MnSOD (Sod2) and survivin (BIRC5 [baculoviral IAP repeat containing 5]) (66). In oncology, elevated RelB expression and activity is a commonly observed adaptation exploited by tumours. For example, one group found that 40% of multiple myeloma specimens possess constitutive RelB (67), which drives the up-regulation of pro-survival genes, supporting important roles for the alternative NF-κB pathway in controlling apoptosis. Based on this evidence, we also hypothesized that RelB would suppress smoke-induced apoptosis in the lung. The molecular mechanisms by which RelB may exert its protective abilities in the respiratory system are unclear but may involve interaction with cellular proteins outside of the NF-κB family.

1.5 The Aryl Hydrocarbon Receptor

Recently, cross-talk between RelB and the aryl hydrocarbon receptor (AhR) have been shown to influence inflammatory protein expression (68). The AhR is a member of the basic helix-loop-helix (bHLH) family of transcription factors that has traditionally been described for its role in mediating adverse responses to man-made toxicants such as 2,3,7,8-tetrachlorodibenzo-p-dioxin (TCDD; dioxin) (69). However, a broad range of biochemical and genetic studies have now demonstrated that the AhR is essential for many biological functions, including the suppression of inflammation and apoptosis (70-73). The AhR is normally sequestered in the cytoplasm through association with HSP (heat shock protein) family members. When soluble ligands, such as dioxin, enter the cell they bind to the AhR and induce conformational changes that permit translocation to the nucleus (74). Nuclear AhR then partners with ARNT (AhR nuclear translocator) to bind DNA regions containing unique sequences

referred to as the DRE (dioxin response element). These elements are present in a battery of genes such as detoxifying enzymes Cyp1a1, Cyp1a2, and Cyp1b1 (74). To terminate AhR signalling, another target of this pathway is the AhRR (AhR repressor), which is postulated to block the AhR in a negative feedback loop by competing with the AhR for ARNT binding (75). An increasing number of genes are regulated by the AhR, including genes related to cell survival, proliferation, inflammation, and anti-oxidant responses (70-73). Many of these pathways have recently been demonstrated to be important for protecting against cigarette smoke.

1.5.1 AhR: suppressor of cigarette smoke-induced inflammation and apoptosis

AhR has an increasingly appreciated role in attenuating inflammation in response to cigarette smoke exposure. Using an animal model of smoke exposure, we have demonstrated that $AhR^{-/-}$ mice have significantly higher inflammatory cell recruitment to the lung, particularly neutrophils (72), a hallmark of COPD that can contribute to the lung parenchymal destruction that underlies airspace enlargement (16). We have also identified the AhR as a suppressor of smoke-induced apoptosis in mouse lung fibroblasts *in vitro* (**Figure 2**). Although the mechanism accounting for this phenomenon was not fully understood, it may be due to a regulation of the antioxidant machinery such as Sod2 (71). Based on the overlapping functions of RelB and AhR in suppressing cigarette smoke-induced damage, it is reasonable to hypothesize that these two proteins comprise a signalling pathway for this end.

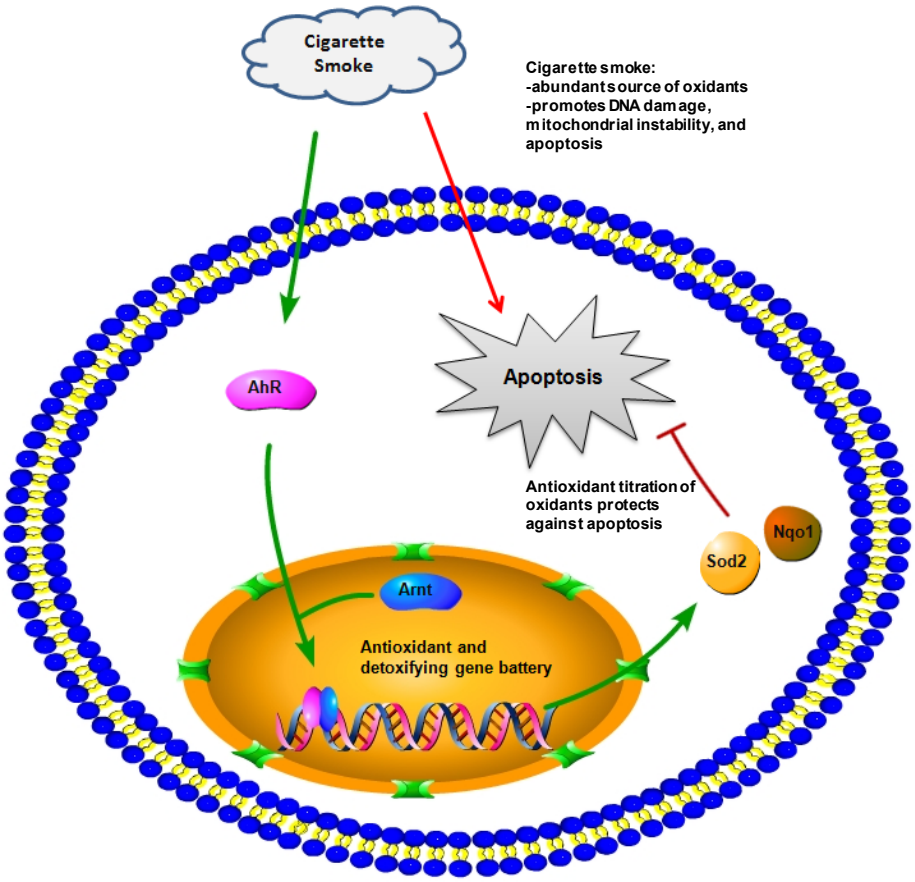

Figure 2. **Scheme of AhR pro-survival signalling.** The AhR suppresses cigarette smoke-induced apoptosis by activation of detoxifying and antioxidant genes, including Sod2 and Nqo1. These factors act to titrate the excessive ROS/RNS generated by cigarette smoke and promote cell survival.

1.5.2 AhR and RelB crosstalk

There is a growing body of literature supporting crosstalk between AhR and RelB. Vogel *et al* observed that AhR and RelB physically interact to regulate the expression of inflammatory genes such as IL-8 in macrophages (76). In particular, this group found that these genes contain a particular sequence in their promoter termed the "RelBAhRE", recognized by the AhR:RelB dimer (76). Upon stimulation with compounds such as forskolin (FSK), AhR preferentially binds RelB, as opposed to ARNT, diverting AhR signalling away from DRE-containing target genes such as Cyp1a1, and towards inflammatory RelBAhRE-containing genes including IL-8 (76). We have published that AhR-deficient lung fibroblasts exposed to cigarette smoke rapidly decrease RelB protein expression, suggesting that the AhR regulates RelB expression (68). While together these findings support a relationship between the AhR and RelB, there is currently no information on the role of RelB in apoptotic cell death in the lung or whether a RelB/AhR partnership promotes lung structural cell health in response to respiratory toxicants such as cigarette smoke. It is also noteworthy that Vogel further demonstrated canonical NF-κB binding to the AhR gene in order to mediate its transcription (77). However, no evidence has so far emerged regarding the capacity of RelB to regulate the expression and activity of the AhR. We therefore explored the role of RelB in regulating cigarette smoke-induced apoptosis and the molecular mechanisms underpinning its relationship with the AhR.

CHAPTER 2: HYPOTHESIS AND AIMS

HYPOTHESIS

We hypothesized that RelB attenuates cigarette smoke-induced apoptosis via regulation of AhR expression and activity.

SPECIFIC AIMS:

AIM 1. Determine if loss of RelB promotes cigarette smoke-induced apoptosis in lung fibroblasts.

AIM 2. Determine if RelB regulates the AhR as a mechanism of promoting cell survival upon cigarette smoke exposures.

CHAPTER 3: EXPERIMENTAL PROCEDURES

3.1 Chemicals

All chemicals were purchased from Sigma (St. Louis, MO) unless otherwise indicated. Actinomycin D (ActD) was purchased from Biomol (Plymouth Meeting, PA).

3.2 Animals

RelB-knockout mice ($RelB^{-/-}$; C57BL/6-RelbTg(H2-K1/GH1)106Bri/J) were obtained from Jackson Laboratory (Bar Harbor, ME), bred in-house at the Meakins-Christie Laboratories (Montreal, QC) and maintained on an ad libitum diet. Lungs from $RelB^{-/-}$ mice and littermate wild-type ($RelB^{+/+}$) controls were harvested for protein expression analysis or generation of lung fibroblasts.

3.3 Cell Culture

Lung fibroblasts were generated from $RelB^{+/+}$ and $RelB^{-/-}$ mice (age 3-4 weeks) using a tissue explant technique as previously described (78) and cultured under standard conditions (71). For all experiments, cells were plated at equal densities and cultured until approximately 90% confluent. Lung fibroblasts generated from at least two different mice of each genotype were used for the majority of experimental analyses.

3.4 Preparation of Cigarette Smoke Extract (CSE)

Research grade cigarettes (3R4F) with a filter were obtained from the Kentucky Tobacco Research Council (Lexington, KT) and CSE generated as previously described (68,71,79). Briefly, CSE was prepared by bubbling smoke from a cigarette into 15 ml of serum-free MEM,

sterile-filtered with a 0.45-μm filter (25-mm Acrodisc; Pall Corp., Ann Arbor, MI). An optical density of 0.65 (320 nm) was considered to represent 100% CSE (71). This CSE preparation was diluted to the appropriate concentration in serum-free MEM to between 2-5%; these concentrations have previously been shown by us to incite apoptosis in primary lung fibroblasts (44,71).

3.5 Real-Time-PCR (qPCR) Array

Detection and quantification of gene expression between CSE-exposed $RelB^{-/-}$ and $RelB^{+/+}$ fibroblasts was first performed by qPCR array. After exposure to 2% CSE for 6 hours, total RNA was isolated using the Qiagen miRNeasy® Mini Kit according to the manufacturer's instructions (Qiagen, Toronto, ON). RNA quality and quantity were assessed using a Nanodrop1000 spectrophotometer (Thermo Fisher Scientific, Wilmington, DE) and 250 ng of total RNA was reverse transcribed using SuperScript III (Invitrogen). The expression of approximately 84 genes was analyzed by qPCR using a commercial PCR array (Oxidative Stress Array PAMM-014, SA Biosciences). These arrays were selected based on functional groupings of genes associated with antioxidant defence and reactive oxygen species (ROS) metabolism. A representative sample from each exposure regime ($RelB^{-/-}$ media, $RelB^{-/-}$ CSE, $RelB^{+/+}$ media, and $RelB^{+/+}$ CSE) was randomly selected for the array. The threshold and baseline were set manually according to the manufacturer's instructions and analysis was carried out using the RT^2 Profiler PCR Array Data Analysis Version 3.4. The relative level of mRNA expression for each gene in each sample was first normalized to the expression of two housekeeping genes (β-Actin and GAPDH) and then normalized to the level of mRNA in the air-exposed sample ($RelB^{-/-}$ or $RelB^{+/+}$). Values represent fold-regulation between media- and CSE-exposed cells based on RelB

expression of those genes having a greater than 4-fold change in relative expression levels.

3.6 Analysis of Gene Expression by qRT-PCR

Total RNA was isolated from media- or CSE-treated $RelB^{+/+}$ and $RelB^{-/-}$ fibroblasts using a Qiagen miRNeasy kit (Qiagen Inc., Valencia, CA) according to the supplier's protocol. RNA was eluted in 30 µl RNase-free water and RNA content and purity was measured using a Nanodrop. Reverse transcription of total RNA was carried out in a 25-µl reaction mixture by iScript II™ Reverse Transcription Supermix (Bio-Rad Laboratories, Mississauga, Ontario) at 25°C for 5 min and 42 °C for 30 min. The mRNA levels of target genes were then analyzed using this cDNA template and gene-specific primers (**Table 2**). qPCR was performed with 1 µl cDNA and 0.5 µM primers added in Ssofast™ Eva Green® Supermix (Bio-Rad) and PCR amplification was performed using a CFX96 Real-Time PCR Detection System (Bio-Rad). Thermal cycling was initiated at 95 °C for 30 s and followed by 39 cycles of denaturation at 95 °C for 5 s and annealing for 5 s. Gene expression data were analyzed using the ΔΔCt method and results are presented as fold-changes normalized to β-Actin.

Table 2.primer sequences used for qRT-PCR analysis

Gene	Forward Primer Sequence	Reverse Primer Sequence
Cyp1a1	CCT TAC CAA GTG CTA GGA TAC AGT CAT AGA	CAG TAA AGA AGA GAG ACC AAG AGC TGA T
Cyp1b1	AAA ATG TAA AGA CCA GAA GTC CTC CTA CC	AGA AAG CCT CAT CCA GGG CTA TAA A
Nqo1	GCG GCT CCA TGT ACT CTC TTC A	ACG GTT TCC AGA CGT TTC TTC C
Sod2	GACCTGCCTTACGACTATGG	GACCTTGCTCCTTATTGAAGC
AhR	AGC ACC ACT AGA CTG AGG GAT TAA CTTC	AGA GTT TAA AGG GCA AGG AGC TAT G

3.7 Cell Imaging

Hoechst fluorescence: Increased fluorescence of the DNA dye Hoechst is indicative of chromatin condensation, a characteristic of cells undergoing apoptosis (80). Therefore, $RelB^{+/+}$ and $RelB^{-/-}$ fibroblasts were cultured on glass chamber slides and treated with control media or with CSE for 6 hours. Following this, cells were fixed in methanol, incubated with the Hoechst for 15 minutes, coversliped and viewed under the Olympus BX51 microscope (Markham, ON). Photographs were taken using a QImaging® Retiga-2000R camera and analyzed with Image-Pro Plus v. 7.0. MitoTracker®Red CM-H2XRos: $RelB^{+/+}$ and $RelB^{-/-}$ fibroblasts were plated at a density of $1x10^4$ cells/well, allowed to adhere overnight and treated with CSE for 6 hours. Following treatment with CSE, MitoTracker®Red (Molecular Probes) (0.5 μM), a mitochondrion selective dye that accumulates within the mitochondria in a membrane potential-dependent manner (81), was added for an additional 30 minutes at 37^0C. Cells were then rinsed in PBS/0.1% Tween 20 and coverslipped with Vectashield and photographed.

3.8 Caspase-3 activity assay

Equivalent numbers of fibroblasts were cultured in a 96-well clear-bottom plate, allowed to adhere overnight, and treated with control media, CSE, or Actinomycin D for 6 h. Caspase-3 activity was measured using a commercially available fluorometric kit as described (71).

3.9 Western Blot

Fibroblasts were grown to approximately 90% confluence and provided with serum-free MEM 18 hours prior to treatment. Total cellular protein was prepared using RIPA lysis buffer (Thermo Scientific, Rockford) and 2-10 μg of protein were fractionated on SDS-PAGE gels and

transferred onto Immuno-blot PVDF membranes (Bio-Rad Laboratories, Hercules, CA) as described (82). Antibodies against RelB (1:2000; Cell Signalling), cleaved caspase-3, cleaved PARP (1:1000; Cell Signalling Technologies) and Actin (1:50000, Millipore, Temecula, CA) were diluted in 2.5% non-fat milk in PBS-Tween (0.1%) and incubated at 4^{o}C overnight. Secondary antibodies were horseradish peroxidise-conjugated goat anti-rabbit IgG (1:10000, Santa Cruz, Santa Cruz, CA) and ZyMax™ horseradish peroxidise-conjugated rabbit anti-mouse IgG (1:10000, Invitrogen, Carlsbad, CA). Detection of protein expression was catalyzed by Clarity™ western ECL substrate (Bio-Rad, Mississauga, Ontario) or Amersham™ western ECL substrate (GE Healthcare, Italy) and imaged using a ChemiDoc™ XRS+ System (Bio-Rad). Densitometric analysis was performed using ImageJ. Protein expression was normalized to Actin and the data are presented as the fold-change relative to the wild-type untreated condition.

3.10 RelB-siRNA knock-down in lung fibroblasts

To confirm the role of RelB in primary lung fibroblasts, siRNA-mediated knock-down was performed. Control mouse lung fibroblasts were seeded at $2x10^4$ cells/cm^2 and transfected with 40 nM of siRNA against RelB (Santa Cruz, sc-36403) or non-targeting control siRNA (Santa Cruz, sc-37007). Transfections were performed according to manufacturer's instructions. Six hours after the transfection, the cells were switched to serum free MEM medium. On the next day, the cells were treated with serum-free medium for 20h, followed by exposure to CSE. Verification of RelB knock-down was done by western blot within 72 hours after transfection.

3.11 Bioinformatic search for RelB binding sites

To investigate whether RelB could be binding to the AhR gene as a mechanism of its

regulation we performed a bioinformatic search of RelB consensus binding sites. e-Ensembl was used to generate a sequence of both intron and exon sequences of the AhR mouse gene. We utilized the alternative NF-κB consensus binding site discovered by Bonizzi *et al* (53) in mice, for our search in the AhR gene. Based on the flexibility of the sequence, our initial search utilized the sequence "GGAGA". To increase the specificity, we manually searched the results and identified those that possessed the greatest consensus to the initial RelB binding site. Overall, this approach generated 4 candidates for RelB binding, designed I-IV. Primers were designed to flank each of these consensus binding sites by approximately 200bp. Primers coding for the promoter region of Actin were used as a negative control to validate the specificity of our RelB antibody.

Table 3. Primer sequences utilized for ChIP assays.

ahrIF	*AAGGCAACTCTCAGCAGGAT*
ahrIR	*TGACAACAGGAAAGTGGGAA*
ahrIIF	*TAGGACTTGCTGTGTGCTGG*
ahrIIR	*AGCTGCTTGTCCGGAGACTA*
ahrIIIF	*CAGTGCTTGTGCCTTTACGA*
ahrIIIR	*CCATCATGCATGTGTGTGAA*
ahrIVF	*TGCTGCAGTTTTTGTCTTGG*
ahrIVR	*ACGCCTCTCTCTGAAGACCA*

3.12 Chromatin Immunoprecpitation (ChIP) Assays

ChIP assays were performed by culturing $RelB^{+/+}$ mouse lung fibroblasts under standard conditions. Cells were then transferred to serum-free conditions for 18 hours and fixed with 1% formaldehyde for 10 minutes. Afterwards, they were collected and lysed with a cell lysis buffer (0.3% HEPES; 1.26% KCL; 2% IGEPAL CA630; pH=8.5) and nuclear lysis buffer (1.22% TRIS; 0.58% EDTA; 2% SDS; pH=8.0). Lysates were then sonicated (15 cycles x 10 sec on; 30

sec off) to achieve fragmentation of ~200-500bp (confirmed by agarose gel electrophoresis). IP fractions were prepared by adding either 5µg of RelB antibody (Santa Cruz C-19) or 5µg of non-specific IgG antibody (Santa Cruz SC-2027). Input fractions were prepared from 10 µL of sonicated lysate. Both IP and input fractions were then reverse cross-linked and extracted for DNA (Favorgen kit: FAGCK001-1). Finally, all DNA sequences were analyzed with qPCR using a thermocycle program of: 95°C 5:00; 45x (95°C 0:10; 58°C 0:10; 72°C 0:10).

3.13 *Statistical Analysis*

Statistical analysis was performed using GraphPad Prism 6 (v. 6.02; La Jolla, CA). A two-way analysis of variance (ANOVA), followed by a Newman-Keuls multiple comparisons test, was used to assess differences between groups defined by two variables. Groups of two were analyzed by student's two-tailed unpaired t-test. Results are expressed as the mean ± SEM of the fold-changes compared to control cells at baseline or control IgG antibody for ChIP assays. This approach was utilized as opposed to absolute values to account for differences in exposures of western blot membranes and/or amplifications for qRT-PCR when comparing independent experimental replicates. In all cases, a p value < 0.05 is considered statistically significant.

CHAPTER 4: CONTRIBUTION OF CO-AUTHORS

This thesis is based on my original work and is presented as a manuscript currently in preparation for peer-review and submission. While I conduced the majority of experiments that constitute this thesis, supporting experiments were performed by the co-authors. These include:

1. **Supplemental apoptosis assays**. Additional techniques to support the hypothesis that RelB suppresses cigarette smoke-induced apoptosis were performed by Angela Rico de Souza, Michela Zago and Dr. C Baglole. These included cleaved PARP immunostaining, caspase-3 activity assays, mitochondrial stability assays, and chromatin condensation experiments.
2. **Microarray of RelB-regulated genes**. The microarray comparing $RelB^{-/-}$ mouse lung fibroblasts (MLFs) to control cells and assessing changes in antioxidant genes such as Nqo1 was performed by Dr. C Baglole.
3. **siRNA knockdown of RelB**. RelB was knocked-down in control MLFs and treated with CSE by Angela Rico De Souza, providing complimentary evidence that RelB regulates the AhR; Angela Rico De Souza also treated $RelB^{-/-}$ and control MLFs with CSE to validate that the AhR protein expression is decreased in the former cell population.
4. **Bioinformatics and ChIP assay assistance**. Manuella Bouttier provided assistance for the bioinformatic search of putative RelB binding sites in the AhR gene and the subsequent design of primers flanking these sites; she also offered technical guidance for optimizing the ChIP assays used for this thesis.

CHAPTER 5: RESULTS AND FIGURES

5.1 RelB down-regulation by CSE and elevated levels of cleaved PARP

We have shown that CSE exposure of human lung fibroblasts decreases RelB protein expression via proteolytic degradation (65). As we predict that RelB expression is essential in protecting against smoke-induced apoptosis, we first sought to identify the effect of CSE on RelB expression and consequent induction of apoptotic markers in mouse lung fibroblasts derived from $RelB^{+/+}$ mice. RelB protein expression was significantly decreased in a dose-dependent manner after exposure to CSE (**Figure 3A**). We also measured the expression of the cleaved form of poly(ADP-ribose)polymerase (PARP) as a well-described marker of apoptosis (71,83). There was little evidence of cleaved PARP at baseline or with 2% CSE exposure (**Figure 3B**). However, there was a marked increase upon exposure to 5% CSE **(Figure 3B**). These data support an inverse association between RelB expression and induction of apoptosis by CSE.

5.2 Genetic ablation of RelB increases cleaved PARP in response to CSE and ActD

Our next objective was to determine whether genetic ablation of RelB would have a causative role in promoting smoke-induced apoptosis. To address this, we compared $RelB^{+/+}$ to $RelB^{-/-}$ fibroblasts treated with 0, 2%, and 5% CSE or with Actinomycin D (ActD; an RNA polymerase II inhibitor that causes apoptosis (71)) and first compared whether there was increased levels of cleaved PARP. There was a robust induction in the levels of cleaved PARP in $RelB^{-/-}$ fibroblasts compared to those which express RelB in response to both CSE and ActD (**Figure 4A**; note both the verification of phenotype and CSE-induced decrease in RelB in wild-type cells [compare with Figure 3A]). Densitometric analysis revealed that there was

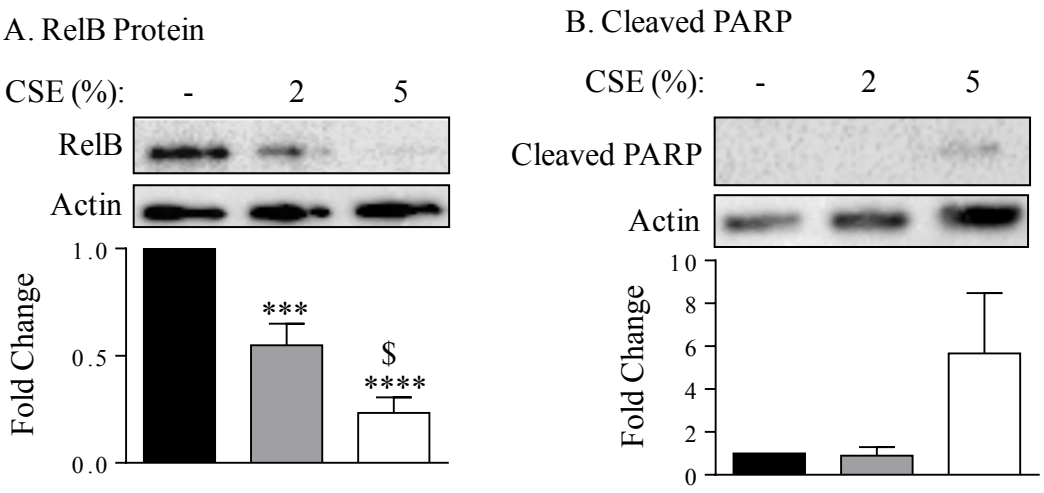

Figure 3. **RelB down-regulation by CSE and association with elevated levels of cleaved PARP**. RelB$^{+/+}$ lung fibroblasts were treated with 0, 2%, and 5% CSE for 6 hours and protein collected for western blot analysis of (*A*) RelB expression or (*B*) cleaved-PARP. Results are expressed as the mean ± SEM normalized to Actin and depicted blots are representative of at least 3 independent experiments. Quantification was performed using Image J and statistical analysis via GraphPad Prism two way-ANOVA test.

significantly higher cleaved PARP in RelB$^{-/-}$ cells at baseline (**Figure 4B**). The increased cleaved PARP was evident in RelB$^{-/-}$ fibroblasts compared to RelB$^{+/+}$ cells in response to CSE (**Figure 4C**). Exposure to ActD increased cleaved PARP in both RelB$^{+/+}$ and RelB$^{-/-}$ fibroblasts, with the induction being significantly higher in RelB$^{-/-}$ fibroblasts (**Figure 4D**). These results were verified by immunofluorescence detection of cleaved PARP, where there is a striking increase in nuclear fluorescence upon exposure of RelB$^{-/-}$ fibroblasts to CSE and ActD, whereas fluorescence was largely lacking in RelB$^{+/+}$ cells (**Figure 4E**).

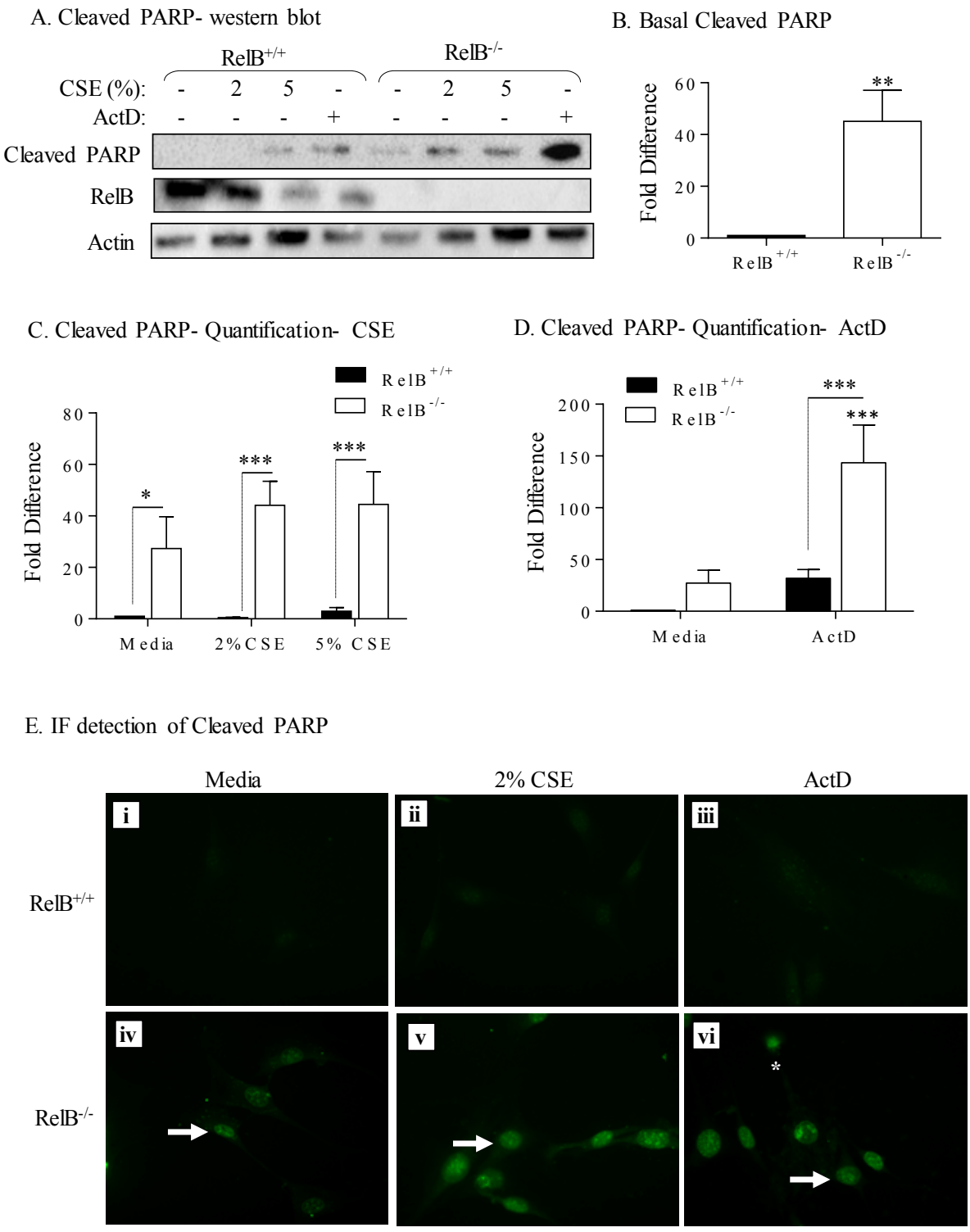

Figure 4. **Genetic ablation of RelB increases cleaved PARP in response to CSE and ActD**. *A,* Cleaved PARP- western blot: There was a noticeable increase in cleaved PARP in RelB$^{-/-}$ fibroblasts exposed to CSE and ActD. Note the decrease in RelB protein levels with increasing

percentages of CSE in $RelB^{+/+}$ cells. Representative western blot is shown. *B,* Basal cleaved-PARP: There was significantly more basal cleaved PARP in $RelB^{-/-}$ cells compared to $RelB^{+/+}$ cells. Results are expressed as the mean ± SEM of 8 independent experiments (** $p < 0.01$). *C,* Cleaved PARP Quantification- CSE: There was significantly more cleaved PARP in $RelB^{-/-}$ cells compared to $RelB^{+/+}$ cells treated with CSE. Results are expressed as the mean ± SEM of 4-6 independent experiments (* $p < 0.05$; *** $p < 0.001$). *D,* Cleaved PARP quantification- ActD: There was significantly more cleaved PARP in $RelB^{-/-}$ cells exposed to ActD compared to media only or ActD-exposed $RelB^{+/+}$ cells. Results are expressed as the mean ± SEM of 4-6 independent experiments (*** $p < 0.001$). *E,* IF detection of cleaved PARP: $RelB^{-/-}$ fibroblasts (*panels iv-vi*) exhibited nuclear cleaved PARP in the absence of CSE (*panel iv- untreated, arrow*). Exposure to 2% CSE or ActD resulted in an apparent increase in cleaved PARP (*panels v* and *vi, arrows*). There was negligible cleaved PARP in lung fibroblasts from $RelB^{+/+}$ mice (*panels i-iii*).

5.3 Genetic ablation of RelB increases cleaved caspase-3 expression and activity

Changes in cellular morphology associated with apoptosis are the result of caspase activation. Caspase-3 is a key mediator of apoptosis, and activation of caspase-3 results in catalytic processing, yielding smaller molecular weight fragments (84). Therefore, we next evaluated the expression levels of cleaved caspase-3 in response to CSE or ActD. In RelB-expressing cells, cleaved caspase-3 was evident following exposure to ActD (**Figure 5A**). In $RelB^{-/-}$ fibroblasts, basal cleaved caspase-3 was readily detectable and appeared to be increased following exposure to 5% CSE and ActD (**Figure 5A**). Densitometric analysis revealed that there was a robust and significant difference in cleaved caspase-3 between $RelB^{+/+}$ to $RelB^{-/-}$ fibroblasts (**Figures 5B** and **5C**). To validate these data, we then utilized an *in vitro* enzyme activity assay that uses a fluorescent, selective caspase-3 substrate (DEVD-AFC); cleavage of this substrate by caspase-3 yields a shift in fluorescence. There was significantly more basal caspase-3 activity in $RelB^{-/-}$ lung fibroblasts compared to RelB-expressing cells (**Figure 5D**). Exposure of $RelB^{-/-}$ cells to CSE (2 or 5%) resulted in a decline in caspase-3 activity when compared to media-only cells. However, caspase-3 activity remained higher when compared to CSE-exposed wild-type cells (**Figure 5D**). ActD increased caspase-3 activity more in $RelB^{-/-}$ cells compared to RelB-expressing cells.

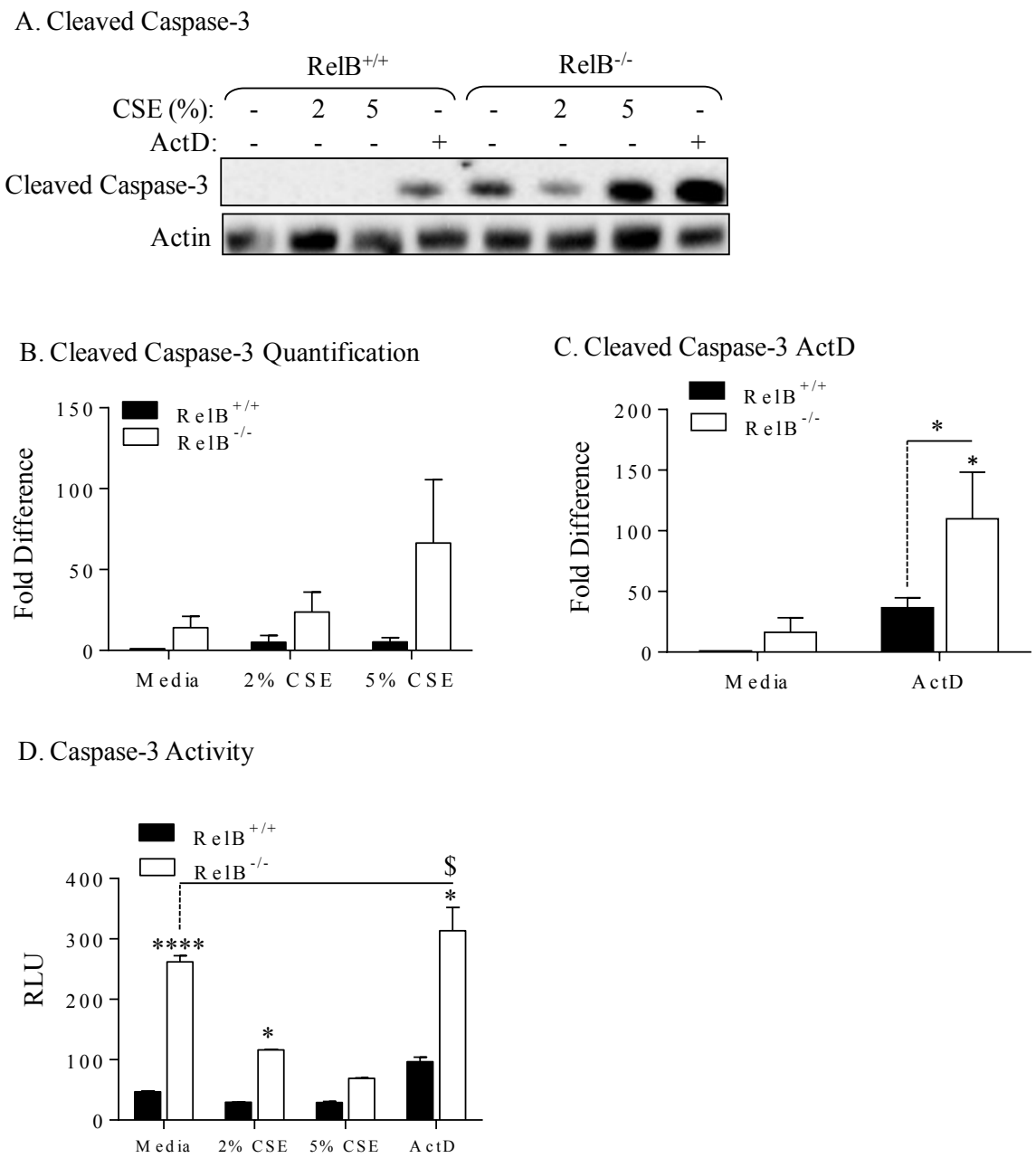

Figure 5. **Genetic ablation of RelB increases cleaved caspase-3 expression and activity.** *A,* cleaved caspase-3: RelB$^{-/-}$ fibroblasts exhibited higher basal levels of cleaved caspase-3 compared to RelB$^{+/+}$ cells. CSE (5%) and ActD (5 μg/ml) dramatically increased cleaved caspase-3 in RelB$^{-/-}$ fibroblasts; these were marginally increased in the RelB-expressing cells. Representative western blots are shown. *B,* Cleaved caspase-3 Quantification: There was a robust increase in cleaved caspase-3 in RelB$^{-/-}$ fibroblasts. Results are expressed as the mean ± SEM of 3 independent experiments. C, Cleaved caspase-3 ActD: There was significantly more cleaved caspase-3 in ActD-exposed RelB$^{-/-}$ fibroblasts. Results are expressed as the mean ± SEM of 4

independent experiments (* $p < 0.05$). *D,* Caspase-3 activity: Caspase-3 activity was assessed using a fluorimetric kit as described in Experimental Procedures. There was a significant increase in caspase-3 activity in $RelB^{-/-}$ fibroblasts compared to $RelB^{+/+}$ cells (* $p < 0.05$; **** $p < 0.0001$ compared to RelB-expressing cells; $ $p < 0.05$ compared to media-only treated cells).

5.4 RelB promotes mitochondrial stability and attenuates chromatin condensation upon exposure to CSE

To further compliment these results, we performed additional imaging analysis for alterations in mitochondrial stability and chromatin condensation, two morphological features of the apoptotic pathway. Cigarette smoke causes apoptosis in lung fibroblasts via the intrinsic apoptotic pathway (44) that results from an intracellular cascade of events leading to mitochondrial membrane permeabilization and subsequent loss of mitochondrial membrane potential ($\Delta\Psi_m$) (85). Given that RelB is implicated in cell survival (66), we first assessed whether RelB suppresses cigarette smoke-induced mitochondrial dysfunction using MitoTracker®Red, a mitochondrion-selective dye that accumulates in the mitochondria in a membrane potential-dependent manner (80); the use of MitoTracker®Red as an indicator of changes in $\Delta\Psi_m$ has been described (71,86). In media-treated $RelB^{+/+}$ lung cells, staining was evident as punctuate cytoplasmic fluorescence, indicative of selective uptake of MitoTracker®Red by healthy and active mitochondria. A similar punctuate cytoplasmic pattern was observed in RelB-deficient fibroblasts (**Figure 6A**, *Media (i and ii*)). Exposure to CSE did not alter this staining pattern in fibroblasts which express RelB (**Figure 6A**, panel *iii*). In $RelB^{-/-}$ fibroblasts, CSE resulted in a dramatic loss of punctuate staining and more diffuse cytoplasmic staining (**Figure 6A**, panel *iv*), indicative of reduced uptake of MitoTracker®Red, supporting that RelB protects against mitochondrial dysfunction due to cigarette smoke exposure.

Finally, we evaluated chromatin condensation, a characteristic of cells undergoing apoptosis that results in nuclei that have compact and simple shapes (87). Increased fluorescence

of the DNA dye Hoechst is indicative of chromatin condensation (79). The majority of lung fibroblasts that were treated with media only had nuclei that were spherical to ovoid in shape with minimal fluorescence (**Figure 6B**, *panels i* and *ii*). It is noteworthy that numerous media-

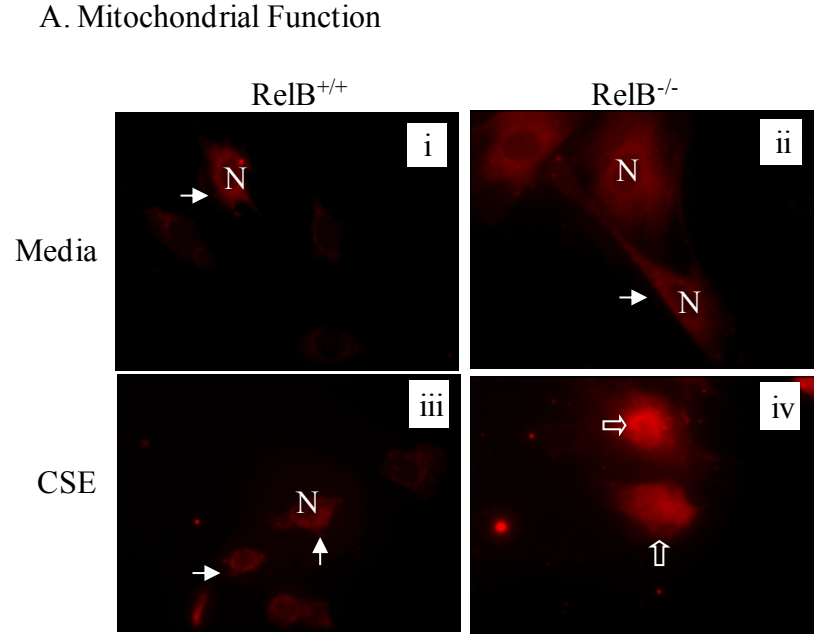

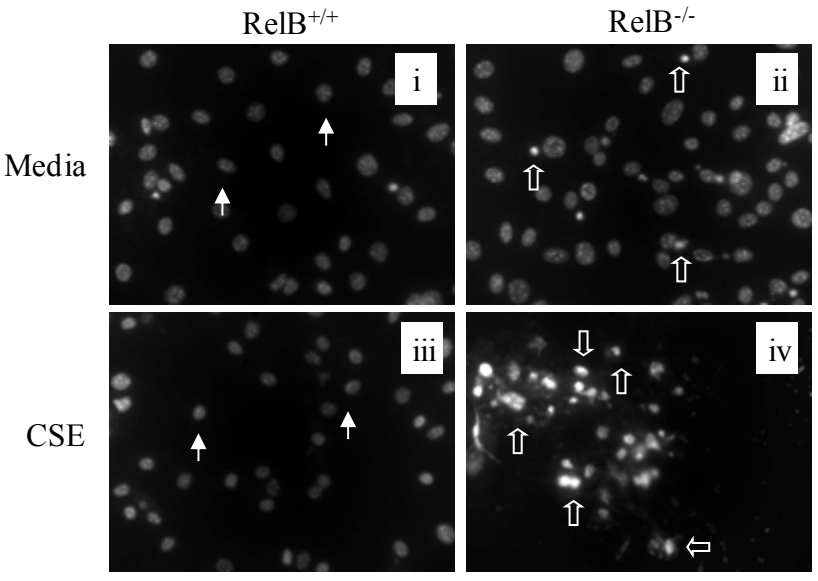

Figure 6. **RelB promotes mitochondrial stability and attenuates chromatin condensation upon exposure to CSE**. *A,* Mitochondrial function: Media-exposed $RelB^{-/-}$ pulmonary fibroblasts (*panel ii*) or $RelB^{+/+}$ cells (*panel i*) exhibited punctuate cytoplasmic fluorescence (*arrows*). No fluorescence was observed in the nuclei (N). This same cytoplasmic distribution was observed in $RelB^{+/+}$ fibroblasts treated with 2% CSE (panels *iii*). In contrast, exposure of $RelB^{-/-}$ fibroblasts to CSE resulted in diffuse cytoplasmic fluorescence (panel *iv*, *open arrows*). *B,* Chromatin Condensation: In pulmonary fibroblasts that are treated with control media, most of the cells have nuclei that are oval with minimal fluorescence (*panels i* and *ii*). Note that there were more $RelB^{-/-}$ fibroblasts with smaller, brightly fluorescent nuclei in the absence of CSE (*panel ii- Media- arrows*). There was a dramatic increase in the number of cells exhibiting chromatin condensation (*panel iv- arrows*) in fibroblasts that lack RelB expression upon exposure to 2% CSE. Note that the nuclei remain unchanged in CSE-exposed $RelB^{+/+}$ fibroblasts (*panel iii*). Magnification = 40x. Images are representative of at least two separate experiments.

only $RelB^{-/-}$ lung fibroblasts exhibited nuclei that were smaller in size with brighter fluorescence (**Figure 6B-** *panel ii*, *arrows*). RelB-deficient fibroblasts exposed to 2% CSE for 6 hours exhibited a dramatic increase in nuclear fluorescence intensity, indicative of chromatin condensation and impending apoptotic cell death (**Figure 6B-** *panel iv*, *arrows*). In contrast, 2% CSE had negligible effect on chromatin condensation in $RelB^{+/+}$ fibroblasts, with the majority of cells maintaining nuclei with compact, spherical shapes (**Figure 6B-** *panel iii)*. When considered as a whole, these results implicate RelB as a key suppressor of apoptosis against cigarette smoke in lung structural cells.

5.5 RelB-deficient cells display a decreased capacity in the induction of antioxidant genes in response to CSE

The mechanism by which RelB protects against cigarette smoke-induced cell death is not known but we predicted this may involve the transcriptional up-regulation of key pro-survival and/or anti-oxidant genes such as Sod2 and survivin (Birc5) (66,88). Therefore, to further examine the mechanism by which RelB suppresses cigarette smoke-induced apoptosis, we treated $RelB^{+/+}$ and $RelB^{-/-}$ cells with media only or with 2% CSE for 6 hours and performed a qPCR array on select genes related to the antioxidant response. Included amongst these were

genes whose induction was associated with RelB expression, including survivin and Sod2. Out of the total number of genes on the array, the expression of 11 genes were up- or-down-regulated at least 4-fold in CSE-exposed control or $RelB^{-/-}$ fibroblasts (**Table 4**). Interestingly, Sod2 mRNA was not noticeably altered by 2% CSE exposure in either $RelB^{+/+}$ or $RelB^{-/-}$ fibroblasts. While several genes were decreased (Gpx4, Gstk1 and Nox4) or increased (Cat and Srxn1) by exposure to 2% CSE, this appeared to be independent of RelB (**Figure 7**). Of the genes examined, Nqo1 exhibited the largest differential fold-change based on RelB expression. Here, exposure of $RelB^{+/+}$ fibroblasts to 2% CSE for 6 hours resulted in a 45-fold increase in Nqo1 (**Table 4** and **Figure 7**). However, in $RelB^{-/-}$ cells, the fold-regulation was dramatically less, with an approximately 8-fold increase. To the best of our knowledge, these data are the first to show regulation of Nqo1 expression by RelB.

Table 4. Gene expression changes in pulmonary fibroblasts derived from RelB$^{-/-}$ and RelB$^{+/+}$ mice exposed to CSE for 6 hours. Values represent fold-regulation compared to media-only cells and are normalized to the housekeeping genes β-Actin and GAPDH.

Gene Name	Gene Symbol	Gene Bank	FOLD REGULATION *Relb*$^{-/-}$	*Relb*$^{+/+}$
Amyotrophic lateral sclerosis 2 (juvenile) homolog (human)	Aqr	NM_028717	-5.5	3.2
Catalase	Cat	NM_009804	1.8	4.9
Copper chaperone for superoxide dismutase	Ccs	NM_016892	1.3	4.6
Dual oxidase 1	Duox1	NM_001099297	-4.4	1.2
Glutathione peroxidase 4	Gpx4	NM_008162	-4.4	-2.8
Glutathione S-transferase kappa 1	Gstk1	NM_029555	-3.9	-4.3
NADPH oxidase 4	Nox4	NM_015760	-4.8	-1.2
NAD(P)H dehydrogenase, quinone 1	Nqo1	NM_008706	8.3	45.3
Protein phosphatase 1, regulatory (inhibitor) subunit 15b	Ppp1r15b	NM_133819	-4.8	-2.3
Superoxide dismutase 2, mitochondrial	Sod2	NM_013671	1.2	1.6
Sulfiredoxin 1 homolog (S. cerevisiae)	Srxn1	NM_029688	4.4	7.0
Thioredoxin reductase 1	Txnrd1	NM_015762	-1.3	4.0

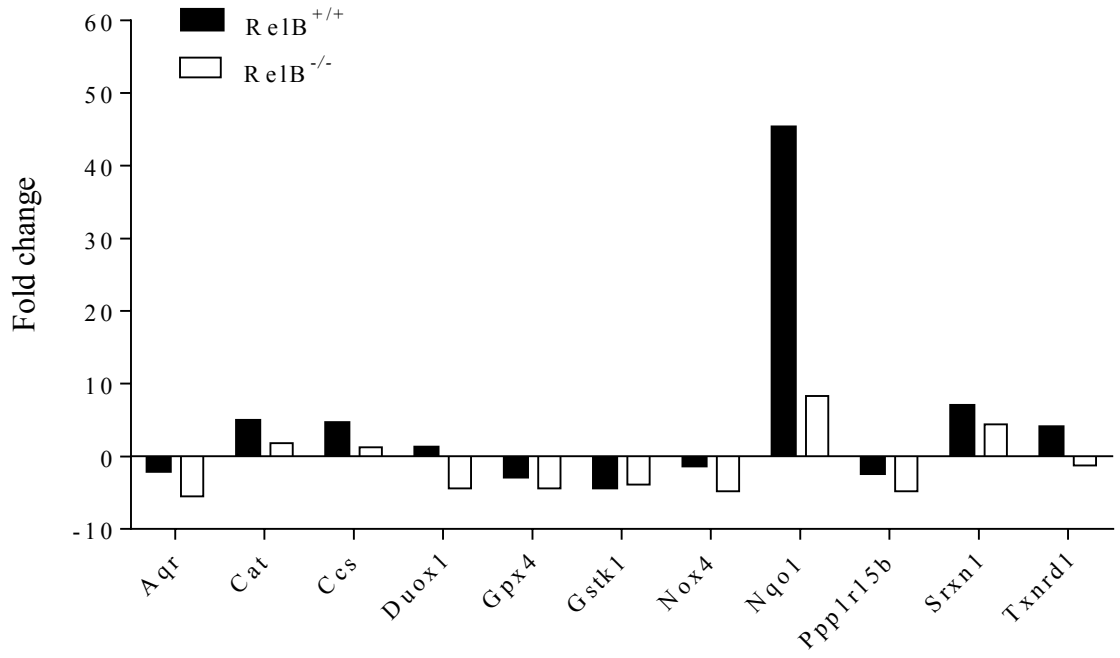

Figure 7. **RelB-deficient cells display a decreased capacity in the induction of antioxidant genes in response to CSE**. RelB$^{+/+}$ and RelB$^{-/-}$ lung fibroblasts were treated with media-only or 2% CSE and cell lysates collected for qPCR analysis of genes related to anti-oxidant defense. Data is presented as a fold change from 2% CSE to baseline in RelB$^{+/+}$ and RelB$^{-/-}$ cells. Note the robust induction of Nqo1 only in RelB-expressing lung fibroblasts.

5.6 RelB promotes the induction of Nqo1 by CSE

Next, we performed qRT-PCR analysis on samples from individual experiments to confirm the expression data obtained from the qPCR array. We included in our analysis those mRNA whose expression was previously linked to RelB (*e.g.*Sod2 and survivin) (66) as well as those not previously associated (*e.g.* Nqo1). There was no significant induction in either survivin or Sod2 mRNA in response to 2% CSE for 6 hours (**Figure 8A** and **8B**). There was also a slight, but not significant difference in survivin mRNA between RelB$^{+/+}$ and RelB$^{-/-}$ fibroblasts (**Figure 8A**) although Sod2 mRNA was significantly lower in RelB-deficient fibroblasts exposed to 2% CSE (**Figure 8B**). Consistent with the qPCR array (**Figure 7**), there was a significant induction

in Nqo1 mRNA expression in response to 2% CSE in RelB$^{+/+}$ fibroblasts; this induction was significant higher in RelB$^{+/+}$ compared to RelB$^{-/-}$ fibroblasts (**Figure 8C**). There was a slight (fold change = 4.6 ± 0.976) but not significant increase in Nqo1 in RelB$^{-/-}$ cells (**Figure 8C**).

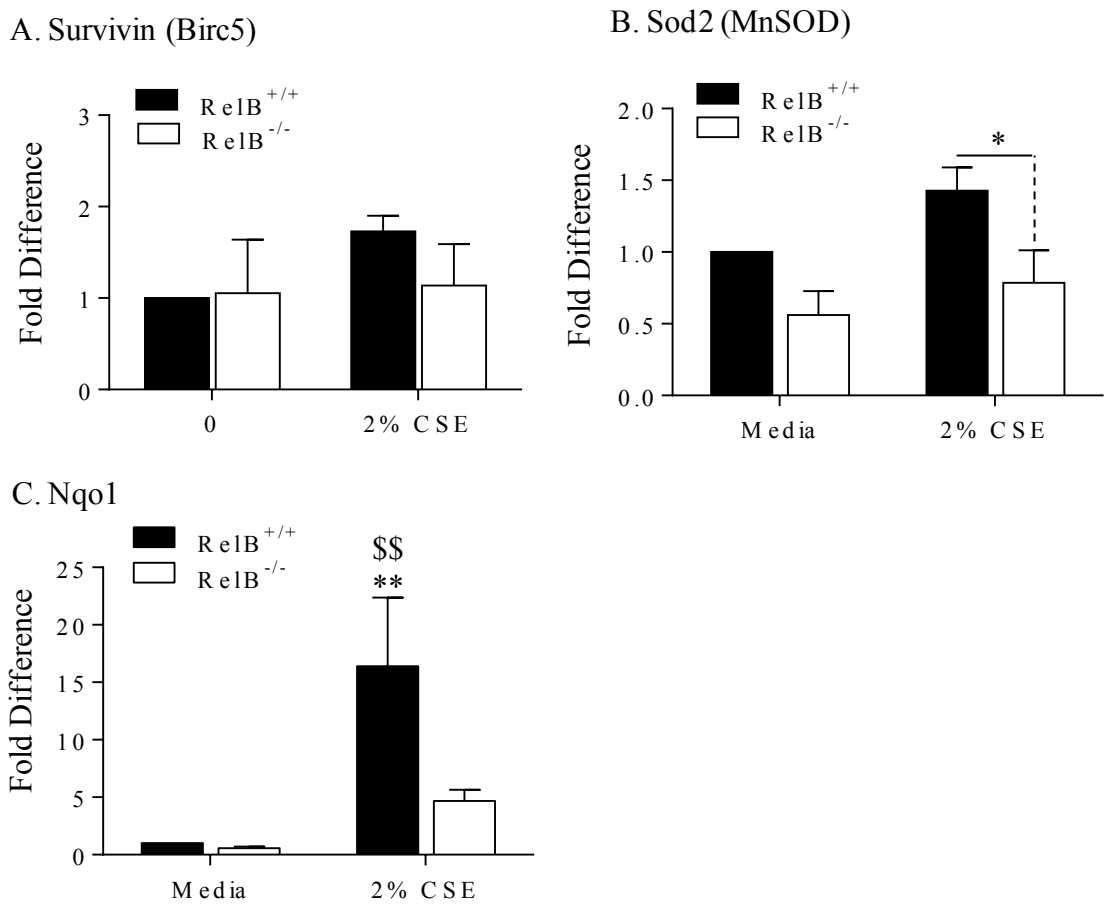

Figure 8. **RelB promotes the induction of Nqo1 by cigarette smoke**. *A,* Survivin (Birc5) - There was a slight, but not significant increase in survivin mRNA when cells were exposed to CSE or based on RelB expression. *B,* Sod2 (MnSOD)-There was significantly less Sod2 mRNA in RelB$^{-/-}$cells exposed to CSE (* $p < 0.05$). *C,* Nqo1- There was a significant increase in Nqo1 mRNA in RelB$^{+/+}$ fibroblasts exposed to CSE for 6 hours (fold change = 16.5 ± 5.6); ** $p < 0.01$ compared to media-only RelB$^{+/+}$ fibroblasts. The induction in Nqo1 mRNA in RelB$^{+/+}$ fibroblasts was significantly greater compared with RelB$^{-/-}$ cells ($ $p < 0.01$). All values were normalized to β-Actin and the results are expressed as the mean ± SEM, n = 10 independent experiments. Fold-regulation was determined by comparison to media-treated RelB$^{+/+}$ fibroblasts.

5.7 RelB regulates the expression of the AhR in vivo and in vitro

The transcription of Nqo1 in response to cigarette smoke can occur through several

signalling pathways, including the AhR. Based on the work of us and others that (1) the AhR suppresses cigarette smoke-induced apoptosis (71) and (2) RelB is an important component in the protective abilities of the AhR (68,71,72), we first investigated whether the mechanism by which RelB suppresses cell death and promotes the induction of Nqo1 was due to regulation of the AhR. First, we evaluated AhR protein expression in lung homogenates from $RelB^{+/+}$ and $RelB^{+/-}$ compared to $RelB^{-/-}$ mice. Intriguingly, we found a significant decrease in AhR protein expression in $RelB^{-/-}$ compared to RelB-expressing mice (**Figure 9A** and **9B**). We next evaluated whether this decrease in AhR was similarly observed in lung fibroblasts derived from these mice. For these analyses, we treated $RelB^{+/+}$ and $RelB^{-/-}$ cells with media only, CSE or benzo[*a*]pyrene (B[*a*]P), an established AhR ligand and component of cigarette smoke (89,90). We found that there was significantly less AhR protein in $RelB^{-/-}$ cells compared to $RelB^{+/+}$ cells (**Figure 9C**). Note that B[*a*]P reduced AhR protein levels in $RelB^{+/+}$ fibroblasts, consistent with proteolytic degradation in response to ligand activation (82). It was interesting to note that this decrease in AhR at the protein level also occurred at the level of the transcript, where there was significantly less AhR mRNA in $RelB^{-/-}$ cells compared to control cells (**Figure 9D**). Exposure of $RelB^{+/+}$ fibroblasts to B[*a*]P also slightly but significantly reduced AhR mRNA (**Figure 9D**). Exposure to CSE also results in loss of AhR protein in lung fibroblasts (**Figure 9E**), consistent with our previous data (71). Finally, to confirm that the effect of RelB deletion on AhR expression was not due to an unknown genetic alteration in the RelB knockout mice that was incidentally unrelated to RelB, we performed siRNA-mediated knockdown of RelB in primary lung fibroblasts and evaluated AhR protein expression by western blot. Here, RelB knock-down resulted in a profound loss of AhR protein (**Figure 9F**). Collectively, these data support that RelB controls the expression of the AhR within structural cells of the respiratory system.

5.8 Genetic ablation of RelB decreases AhR target gene expression

To now confirm whether the loss of AhR in RelB-deficient cells results in a functional and corresponding decline in AhR activity, we first compared the expression of the well-characterized AhR target-genes cyp1a1, cyp1b1 and Nqo1 between $RelB^{+/+}$ and $RelB^{-/-}$ lung fibroblasts exposed to CSE or B[*a*]P. There was negligible cyp1a1 expression in media-only exposed cells, but was induced significantly (> 300 fold) only in $RelB^{+/+}$ cells exposed to 2% CSE or B[*a*]P (**Figure 10A** and **10B**, *black bars*). In contrast, there was no increase in cyp1a1 in $RelB^{-/-}$ cells, and thus cyp1a1 remained significantly lower compared to $RelB^{+/+}$ cells (**Figure 10A** and **10B**). Cyp1b1 mRNA and protein was induced between 2-4 fold by both 2% CSE and B[*a*]P only in $RelB^{+/+}$ cells, with no induction in $RelB^{-/-}$ cells (**Figure 10C**, **10D** and **10E**). Finally, we evaluated the capacity of $RelB^{+/+}$ and $RelB^{-/-}$ cells to increase the expression of Nqo1 in response to B[*a*]P, a well-described AhR ligand. Similarly, there was a significant increase in Nqo1 only in $RelB^{+/+}$ fibroblasts exposed to B[*a*]P (**Figure 10F**). These data confirm that RelB controls the expression and activity of the AhR and supports that RelB regulation of the AhR is key to its protective abilities against excessive apoptosis caused by cigarette smoke.

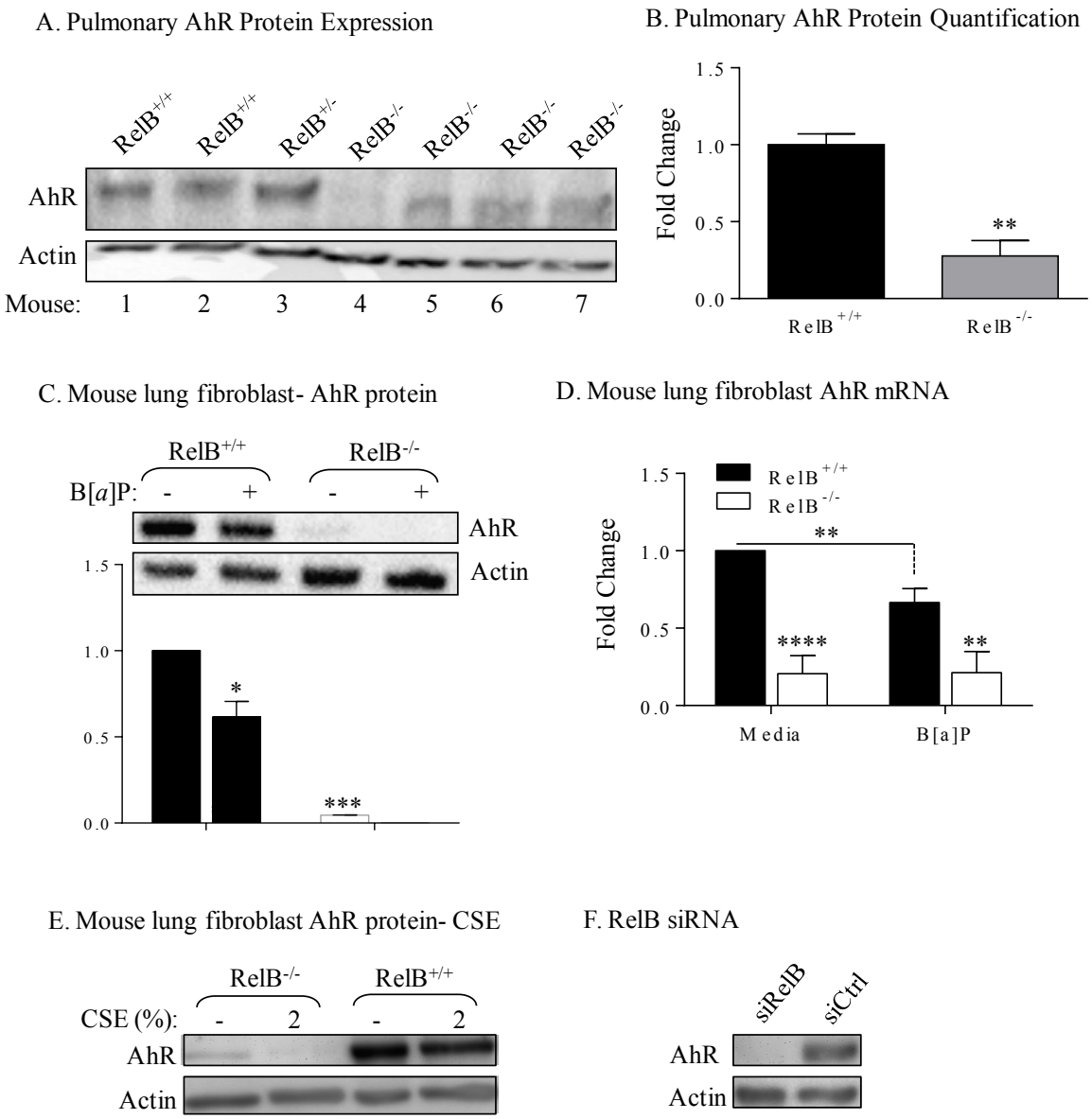

Figure 9. **RelB regulates the expression of the AhR *in vivo* and *in vitro*.** *A,* Pulmonary AhR Protein Expression: Lung homogenate of RelB-expressing and $RelB^{-/-}$ mice were compared for AhR levels by western blot analysis. Three RelB-expressing (a combination of $RelB^{+/+}$ and $RelB^{+/-}$) and 4 $RelB^{-/-}$ mice were analysed. *B,* Pulmonary AhR Protein Quantification- There was significantly less AhR protein in the lungs of $RelB^{-/-}$ mice (** $p < 0.01$); results are expressed as the mean ± SEM. *C,* Mouse lung fibroblasts- AhR protein: $RelB^{+/+}$ and $RelB^{-/-}$ mouse lung fibroblasts were treated with media only or B[*a*]P (0.1μM) for 6 hours and collected for AhR protein. There was significantly less AhR protein in $RelB^{-/-}$ cells (*** $p < 0.001$). Note the decrease in AhR protein in $RelB^{+/+}$ cells exposed to B[*a*]P (* $p < 0.05$ compared to $RelB^{+/+}$ cells exposed to media only). Results are expressed as the mean ± SEM of two independent experiments. *D,* Mouse lung fibroblasts - AhR mRNA: There was significantly less AhR mRNA

in RelB$^{-/-}$ cells compared to RelB$^{+/+}$ cells; B[*a*]P reduced AhR levels only in RelB$^{+/+}$ cells. Results are expressed as the mean ± SEM of 8 independent experiments (** $p < 0.01$; **** $p < 0.0001$). *E,* Mouse lung fibroblast AhR protein- CSE: There was dramatically less AhR protein in RelB$^{-/-}$ cells compared to RelB$^{+/+}$ cells; CSE decreased AhR protein. Representative western blot is shown. *F,* RelB siRNA: knock-down of RelB in control lung fibroblasts resulted in a dramatic loss of AhR protein. Representative western blot is shown.

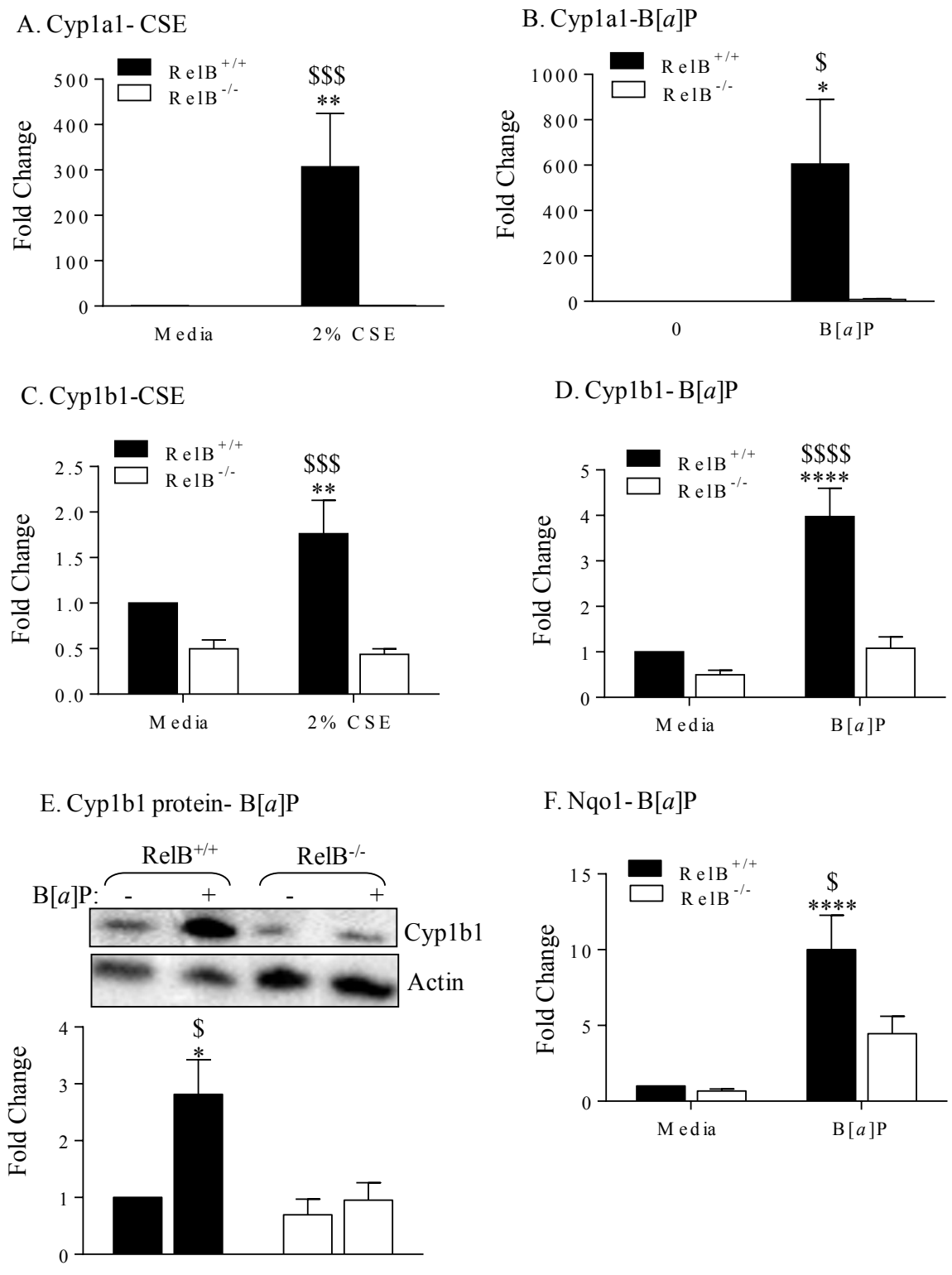

Figure 10. **Genetic ablation of RelB decreases AhR target gene expression**. RelB$^{+/+}$ and RelB$^{-/-}$ mouse lung fibroblasts were treated for 6 hours with media or with 2% CSE or B[*a*]P (0.1μM) and cell lysates collected for RNA or protein analysis of cyp1a1, cyp1B1 and Nqo1. Both 2%

CSE and B[*a*]P significantly increased cyp1a1 (*A, B*) cyp1b1 (*C, D, E,*) and Nqo1 (*F*) only in $RelB^{+/+}$ cells (*p < 0.05, **p < 0.01, **** p < 0.0001 compared to media-only cells; $ p < 0.05, $$$ p < 0.001, $$$ p < 0.0001 compared to CSE or B[*a*]P-exposed $RelB^{-/-}$ fibroblasts). Results are expressed as the mean ± SEM of 3-8 independent experiments. Representative western blot is shown.

5.9 RelB binds to the AhR gene

Based on our observation that $RelB^{-/-}$ fibroblasts possess significantly lower AhR mRNA, we speculated that RelB may be exerting regulation of the AhR at the transcriptional level potentially by binding to its gene. To test this hypothesis, we performed a bioinformatic search of the RelB consensus binding site identified by Bonizzi *et al* (53) in the AhR mouse gene. Our search yielded 4 putative RelB binding sites, designated I-IV. I was located approximately 2.5kb upstream of the translational start site whereas sites II-IV were located 10kb downstream in an intronic region of the AhR gene (**Figure 11**A). To evaluate RelB binding at these sites, we performed ChIP assays in $RelB^{+/+}$ fibroblasts at baseline. We found that at RelB binding sites I (**Figure 11B**), II (**Figure 11C**) and IV (**Figure 11E**), there was significantly greater enrichment of DNA sequences (~4, 1.5, and 2-fold respectively) from the RelB IP condition compared to the non-specific IgG. To validate the specificity of our RelB antibody we tested the promoter region of Actin and found no significant difference with the IgG antibody.

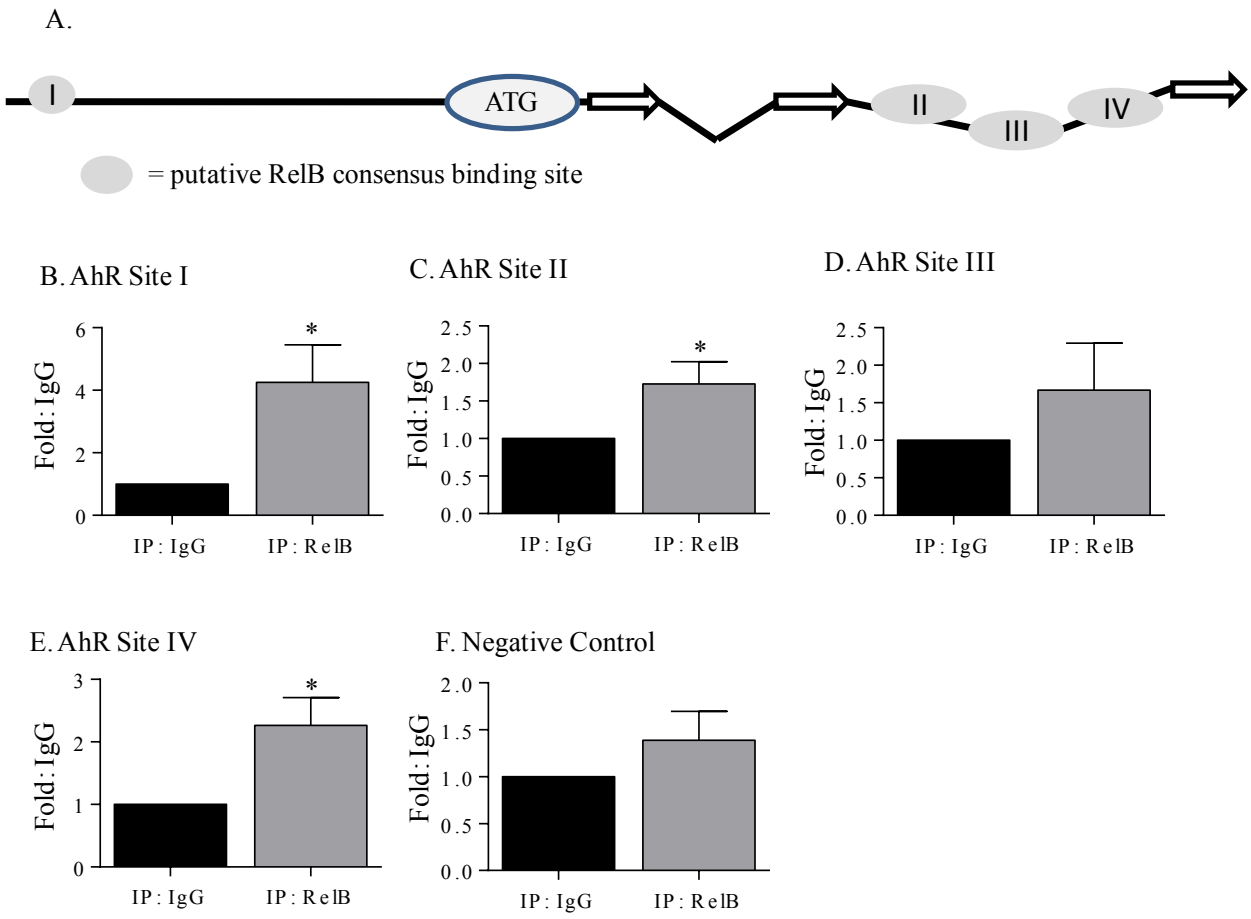

Figure 11. **RelB binds to the AhR gene.** *A,* 4 Putative RelB binding sites were located in the AhR mouse gene, designated I-IV. $RelB^{+/+}$ mouse lung fibroblasts were cultured at baseline and prepared for ChIP assays (see Experimental Procedures) whereby the DNA derived from the RelB and IgG fractions were compared with qPCR for expression at binding sites I-IV. There was significantly greater enrichment of DNA at sites I (*B*), II (*C*), and IV (*E*) whereas III displayed no significant difference (*D*). As a negative control, the promoter region of Actin was amplified and demonstrated no significant difference (*F*). Results are representative of 10 independent experiments, expressed with SEM, and analyzed for statistical significance using a student's t-test.

5.10 Proposed model of RelB suppression of cigarette smoke-induced apoptosis via the AhR

Based on our observations, we propose that RelB protects lung structural cells against cigarette smoke-induced apoptosis by regulating the expression and activity of the aryl hydrocarbon receptor (AhR). Both proteins are requisite for the appropriation of an antioxidant gene battery (e.g. Nqo1 and Sod2) required to titrate the excessive oxidative burden of cigarette smoke, which causes apoptosis (**Figure 12**). The mechanism by which RelB regulates the AhR is incompletely understood but may involve direct transcriptional regulation by binding to its gene.

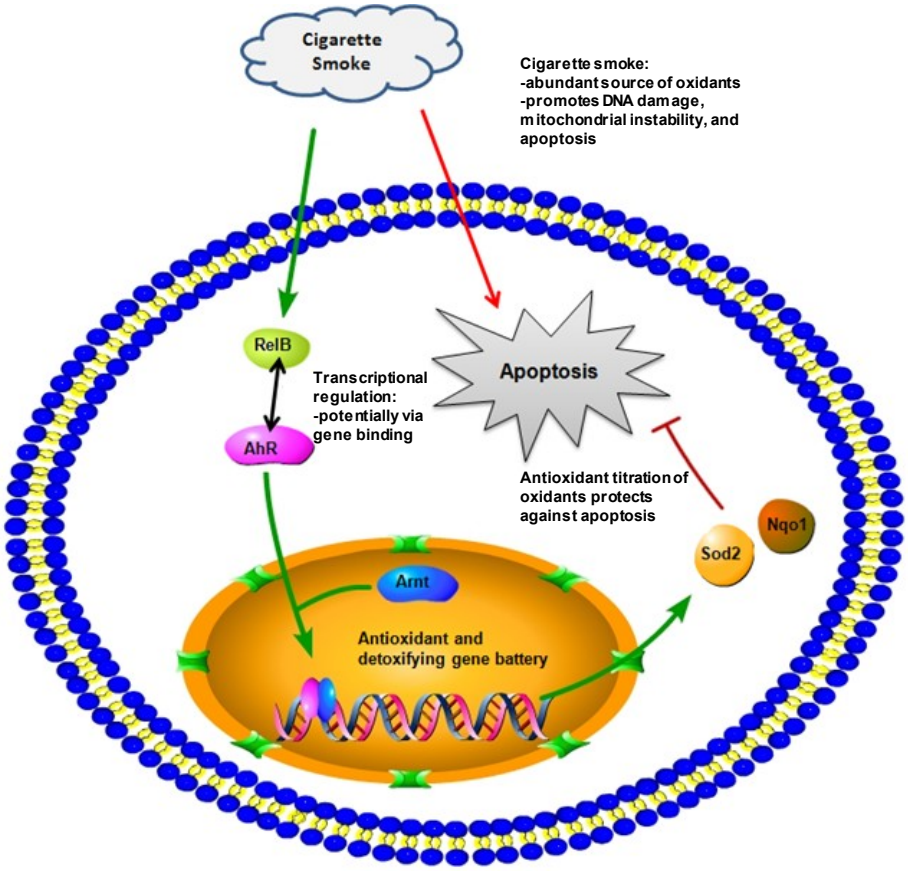

Figure 12. **Proposed model of RelB suppression of cigarette smoke-induced apoptosis via the AhR**. Cigarette smoke induces apoptosis via oxidative stress. RelB regulates the AhR pathway to promote the up-regulation of genes involved in protecting against cigarette smoke-induced apoptosis such as antioxidants Sod2 and Nqo1. The mechanism by which RelB controls the AhR is incompletely understood but may involve transcriptional regulation via gene binding.

CHAPTER 6: DISCUSSION

6.1 COPD: implications of RelB in protecting against cigarette smoke-induced apoptosis

Chronic cigarette smoke exposure remains the predominant cause for the development of many diseases, including lung cancer and COPD, both major health burdens with limited therapeutic options (2,91). However, the mechanism(s) linking smoke inhalation to lung damage are poorly understood. A major hallmark of the emphysematous component of COPD is elevated apoptosis of lung structural cells such as fibroblasts (18). We have previously published on the sensitivity of lung fibroblasts to undergo cigarette smoke-induced apoptosis (44) and that RelB expression is reduced in smokers with and without COPD (65). Combined with knowledge that RelB promotes cell survival in many cell types (66,67,92) led us to explore whether RelB protects lung cells against smoke-induced cell death.

6.2 Mechanisms of cigarette smoke-induced RelB down-regulation

Our first observation revealed that exposure of lung fibroblasts to cigarette smoke reduces cellular RelB protein concomitant with increased cleaved PARP (**Figure 3**). These data are consistent with our recent data showing proteolytic degradation of RelB in human lung fibroblasts due to *in vitro* smoke exposure (65), suggesting that this finding is not specific to mouse. Although the mechanism by which cigarette smoke leads to this loss in RelB levels is unknown, it has been demonstrated that RelB can be degraded upon stimulation of T cells with ionomycin, leading to rapid phosphorylation and subsequent degradation in the proteosome requiring Glycogen Synthase Kinase 3 beta (GSK3β) (93). In particular, it was found that activation of the T-Cell Receptor (TCR) triggered a downstream pathway that phosphorylated RelB at two serine residues in order for targeting to the proteosome. In B cells, RelB can be

similarly degraded via Mucosa-associated lymphoid tissue translocation protein 1 (Malt1), a paracapase protease that cleaves substrate for subsequent degradation in the protesome (94). Taken together, these observations raise the possibility that cigarette smoke similarly induces phosphorylation of RelB that ultimately culminates in proteolytic degradation. The loss of RelB expression may have considerable consequence for COPD progression; given our data demonstrating a role for RelB in suppressing cigarette smoke-induced apoptosis, it is conceivable that a decline in RelB expression may result in exacerbated lung cell death with progressive smoking. Future experiments could be directed towards analyzing components of the proteolytic degradation pathway in our *in vitro* cigarette smoke exposure model. In particular, mouse lung fibroblasts treated with increasing concentrations of CSE can be analyzed for phosphorylation status of RelB, probing residues that result in degradation as reported in the literature. To validate that phosphorylation of these particular residues are required for RelB degradation, flagged RelB constructs can be designed with mutations against these residues and stably transfected into these cells for treatment with CSE to assess RelB expression. Additionally, these cells could be pre-treated with the proteosome inhibitor MG132 to assess whether RelB protein expression can be maintained in the presence of CSE.

Curiously, in conjunction with the loss of RelB with CSE, it is apparent that ActD, a known inducer of apoptosis, also reduced cellular RelB protein expression (**Figure 4A**). Such an observation may raise the possibility that loss of RelB is a feature of a cell already committed to apoptosis rather than its loss contributing towards the induction of the process. However, the decrease in RelB expression even with 2% CSE (**Figure 3A**) coupled with no apparent increase in cleaved PARP at this dosage **(Figure 3B**) does not support this notion. Nevertheless, this experiment itself cannot offer complete insights into the role of RelB in suppressing cigarette

smoke-induced apoptosis and requires additional experimentation whereby RelB expression is manipulated.

6.3 Loss of RelB in promoting cigarette smoke-induced apoptosis

Utilizing lung fibroblasts derived from mice which lack RelB expression, we evaluated markers of apoptosis to ascertain a causative role for RelB deficiency/loss in promoting smoke-induced apoptosis. Using measurements of apoptotic protein expression, assays of mitochondrial stability, and fluorescent imaging of condensed chromatin as an indicator of apoptotic cell death, we demonstrate that RelB suppresses cigarette smoke-induced apoptosis. In fact, we propose that RelB is necessary to promote lung cell survival even in the absence of known apoptotic stimuli. Our data show that $RelB^{-/-}$ fibroblasts displayed elevated apoptosis at baseline (*i.e.* serum-free conditions without CSE or ActD) but that there was further enhancement of apoptosis upon treatment. Many apoptotic indicators such as cleaved caspase-3 were elevated and remained so after smoke and ActD exposure. Although the increase in cleaved-PARP immunostaining (**Figure 4E**) in $RelB^{-/-}$ cells cannot definitively codify these cells as apoptotic, we believe that our chromatin condensation assay (**Figure 6B**) supports the notion that these cells are undergoing this process. It may also be noteworthy that some of our western blots display variability in Actin, our house-keeping gene used as a loading control. We do not believe that the different treatments and/or cell types used here are associated with Actin regulation, however the variation observed may contribute towards the overall accuracy of the densitometry analysis. Nonetheless, we maintain that this limitation is unlikely to confound the interpretation of our results. Interestingly, despite all indication that $RelB^{-/-}$ fibroblasts have higher apoptosis, there was less caspase-3 activity in $RelB^{-/-}$ fibroblasts upon exposure to CSE (**Figure 5D**). It is

possible that CSE may reduce caspase-3 activity due to a direct effect on the active protein, but that the threshold level of activity needed to induce apoptosis is not affected; thus there is no interference with impending apoptosis (95). Caspase-3 activity after exposure to CSE remained significantly higher in $RelB^{-/-}$ fibroblasts, supporting the contention that higher levels due to RelB-deficiency are sufficient to drive the apoptotic process. A western blot of total pro-caspase-3 may be beneficial to demonstrate that the differences in the expression and activity of cleaved caspase-3 in $RelB^{-/-}$ cells are indeed due to elevated apoptosis as opposed to differences in the levels of the precursor enzyme.

Overall our data suggest that enhanced or accelerated loss of RelB galvanizes apoptosis across multiple contexts that may have important implications for emphysema. While at this time we cannot conclude that reduced RelB expression due to smoking facilitates the development of COPD, it raises the possibility that an individual susceptible to COPD (≈ 20% of smokers) may have lower RelB than a smoker who does not go on to develop emphysematous lung destruction (96). Further studies into RelB expression and function in COPD may shed light on the role of the non-canonical NF-κB pathway in smoke-related pathologies.

6.4 RelB and AhR regulation of cigarette smoke-induced apoptosis

One of our more intriguing pieces of data came from explorations related to the mechanism of action by which RelB attenuates apoptosis. Here, we utilized a qPCR array to evaluate the expression of anti-oxidant genes related to cell survival. These data revealed first that Sod2 is a RelB-regulated gene, data that are consistent with the findings of Mineva *et al*. These investigators observed that loss of RelB resulted in decreased Sod2 expression (66). Interestingly, we did not find that RelB regulated Survivin as reported in B cells. This could

reflect potential differences in cell-type and/or experimental models. What was most striking, however, was the dramatic difference in the induction of Nqo1 between RelB$^{-/-}$ and RelB-expressing lung fibroblasts exposed to CSE (**Figures 7-8**). To our knowledge, this is the first indication that there is RelB-dependent induction of Nqo1, an anti-oxidant enzyme whose expression is regulated by nuclear factor erythroid-derived 2-like 2 (Nrf2; NFE2L2) and the AhR (97). Given the relationship between AhR and RelB (44,72,76), we next explored whether RelB regulation of AhR expression and/or activity was associated with the reduction in Nqo1 levels. Our data strongly support that RelB controls the expression, and hence activity, of the AhR, as RelB$^{-/-}$ cells had significantly lower AhR mRNA and protein concomitant with lower induction of the well-characterized AhR target genes cyp1a1 and cyp1b1 (**Figures 9-10**).

Overall, we postulate that RelB is suppressing smoke-induced apoptosis in the lung directly via the AhR. In support of this assumption, we have demonstrated that separately, both the AhR and RelB are essential for suppression of apoptosis (**Figures 3-6** and (71)). Additionally, both the AhR and RelB regulate genes involved in responding to oxidants, such as antioxidants Sod2 and Nqo1, which may play a role in suppressing the potent oxidative burden of cigarette smoke (**Figures 7-8** and (71)). It needs to be highlighted however, that Sod2, unlike Nqo1, was not significantly up-regulated in control cells by CSE **(Figure 8**). This suggests that Sod2 may play a more constitutive antioxidant role, however given that such proteins are required for cell survival (40), it is conceivable that the loss of Sod2 in RelB$^{-/-}$ cells contributes towards their enhanced apoptosis, particularly when treated with CSE. These observations also agree with a recent publication by Zhang *et al*, which demonstrated that the AhR and RelB function together to protect fetal human pulmonary endothelial cells against hyperoxic damage (73).

6.5 RelB regulation of the AhR

The exact mechanism by which RelB controls AhR in lung fibroblasts remains unclear. Both the AhR and RelB interact physically and regulate genes, such as IL-8, in macrophages upon forskolin treatment by binding to a unique promoter sequence called the RelBAhRE (76). Whether both RelB and AhR are needed for optimum induction of Nqo1 in our system remains to be seen. We have shown that the AhR promotes the retention of RelB protein upon smoke exposure (44). Given that cigarette smoke contains AhR ligands that also cause a loss of AhR protein (71,72) it is possible that the AhR also undergoes accelerated degradation without the presence of RelB. To address this possibility, future experiments could utilize cyclohexamide-chase experiments in $RelB^{+/+}$ and $RelB^{-/-}$ mouse lung fibroblasts to halt protein translation and determine whether RelB regulates AhR protein degradation.

However, we do not consider protein stability to be the sole mechanism by which RelB controls AhR expression as our data show that RelB deficiency is associated with significantly decreased AhR mRNA (**Figure 9**). This suggests that RelB is regulating the AhR at the level of transcription. Given that Vogel *et al* demonstrated that RelA binds directly to the AhR promoter to activate gene transcription (77), we sought to investigate whether RelB may behave in a similar capacity. We identified 4 putative RelB consensus binding sites in the AhR mouse gene and evaluated with ChIP assays the ability of RelB to bind to this gene. We demonstrated that RelB binds at 3 of these sites, most pronounced at sites I and IV (see **Figure 11**). However, it needs to be noted that this experiment cannot definitively prove that RelB binding is requisite for optimal induction of the AhR gene. Future experiments aimed towards cloning these sites into luciferase constructs and performing site-directed mutagenesis would be a useful continuation of the work presented here.

It is noteworthy that our data differs with that presented by Vogel *et al.,* who described that RelA- and not RelB- was essential for regulating transcription of the AhR (77). While the reason for this discrepancy is not clear, it is possible that inherent differences in the cell population may be a contributing factor. In our study, we utilized lung fibroblasts from mice aged 3-4 weeks, whereas the study by Vogel and colleagues utilized mouse embryonic fibroblasts (MEFs) (77). It is therefore possible that RelA is the principal regulator of the AhR during this stage of development but that RelB predominates during the post-natal period and/or transition to adulthood. It also remains to be seen whether this is lung and/or fibroblast-specific. Given that the lungs of $RelB^{-/-}$ mice also had significantly less AhR protein (**Figure 9**), we expect that multiple lung cell types (*e.g.* endothelial and epithelial cells) will similarly have reduced AhR expression. Confirmation of this assumption could be done via RelB siRNA knock-down in mouse lung epithelial cell lines, such as MLE-12, followed by assessment of AhR expression and activity to evaluate whether our findings are applicable to additional lung cell types.

6.6 Impact of findings: limitations and possible applications for COPD

One limitation of our experiments is that they alone cannot definitively prove RelB directly attenuates apoptosis in response to cigarette smoke via the AhR. Knock-out of RelB strongly suggests that this protein affords a protective mechanism against this process and regulates the expression and activation of the AhR, but additional experimentation will be requisite to more robustly support our hypothesis. For example, it would be worthwhile to assess the role of RelB activation and localization in affecting smoke-induced apoptosis; co-treatment of MLFs with CSE and RelB activators such as CD40L followed by assessment of apoptosis

may offer additional information regarding the role of RelB activity in this process. Moreover, transfection of $RelB^{-/-}$ MLFs with an AhR plasmid to investigate rescue from smoke-induced apoptosis would further support that the pro-survival pathway of RelB is indeed AhR-dependent as we hypothesize.

Another important limitation of our model, and therefore their implications for COPD, is the experimental model of apoptosis performed *in vitro*, which may not accurately model the complexity of this process *in vivo*. It is well-described that chronic inflammation triggered by smoke leads to the production of secondary ROS that can further perpetuate apoptosis (18). Moreover, the release of metalloproteases from recruited inflammatory cells such as neutrophils can promote apoptosis by destroying extracellular matrix (ECM) components (18). Consequently, our model best evaluates the effects of acute cigarette smoke exposures on structural lung cell survival. While endeavours to assess the role of RelB in inflammation and apoptosis *in vivo* are ongoing, similarities in the pathogenic response between *in vivo* smoke and CSE (98) support the reproducibility of our *in vitro* smoke model to scenarios that might occur *in vivo*. As a result, we predict that the lungs of $RelB^{-/-}$ mice will show significant signs of lung structural cell apoptosis when treated with cigarette smoke.

From a clinical perspective, RelB may be useful as a biomarker for COPD progression. We have previously reported that peripheral RelB expression is significantly correlated with cardiovascular indicators in COPD patients during acute exacerbations (99). To our knowledge neither RelB nor AhR polymorphisms have been reported for COPD. Thus, it remains to be seen whether RelB and/or AhR levels due to specific polymorphisms are novel indicators for emphysematous progression. Further insight into the relationship between AhR and RelB in maintaining lung structural cell health may lead to the development of targeted therapies aimed

at protecting their expression following chronic cigarette smoke inhalation.

6.7 Future directions: dual regulation of AhR by RelA and RelB?

A growing body of evidence suggests that there is cross-talk between NF-κB members RelA and RelB. RelA has been found to regulate the expression of RelB at the transcriptional level (100). In some contexts, RelB attenuates the inflammatory effects of RelA by forming transcriptionally inactive complexes (60). Conversely, it has also been reported that RelA may actually require RelB for proper induction of certain genes, such as granulocyte macrophage colony-stimulating factor (GM-CSF) (101). This latter idea is further supported by previous work from our group that found $RelB^{-/-}$ MLFs displayed significantly less RelA activity using a luciferase NF-κB target gene promoter construct (102). Interestingly, we also observed here that $RelB^{-/-}$ MLFs displayed significantly less RelA mRNA (**Supplementary Figure 1**), suggesting that the deficiency in RelA activity could be due to decreased expression. Further experiments should continue to characterize this possibility. Given that Vogel *et al* reported RelA was required for regulation of the AhR (77), it is conceivable that both RelB and RelA may be requisite for proper regulation of the AhR in lung cells as well. One might envision that RelA and RelB are both recruited to the AhR gene for its proper induction, similar to the mechanism of GM-CSF regulation.

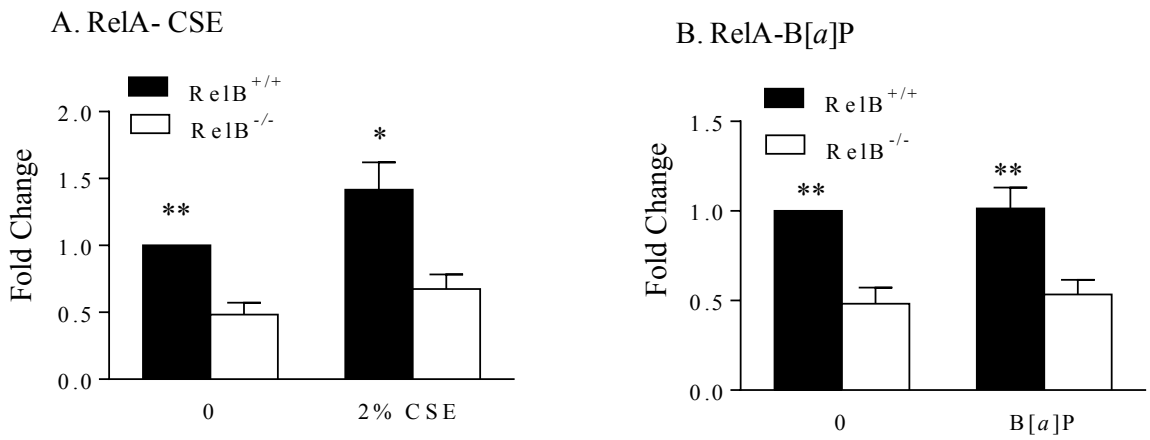

Supplementary Figure 1. **RelB regulates the mRNA expression of RelA**. $RelB^{+/+}$ and $RelB^{-/-}$ cells were treated with and without 2% CSE or B[*a*]P (0.1μM) for 6 hours and analyzed for RelA mRNA. $RelB^{-/-}$ cells displayed significantly less RelA mRNA expression at baseline ($p<0.01$), 2% CSE ($p<0.05$) and B[a]P (<0.01) than control cells. Results are expressed as the mean ± SEM of 7 independent experiments.

CHAPTER 7: REFERENCES

1. Carter, B. D., Abnet, C. C., Feskanich, D., Freedman, N. D., Hartge, P., Lewis, C. E., Ockene, J. K., Prentice, R. L., Speizer, F. E., Thun, M. J., and Jacobs, E. J. (2015) N Engl J Med 372, 631-640.

2. Caramori, G., Kirkham, P., Barczyk, A., Di Stefano, A., and Adcock, I. (2015) Ann N Y Acad Sci 1340, 55-64.

3. Pauwels, Romain A., and Klaus F. Rabe. (2004) The Lancet 364, 613-620.

4. Rodriguez-Roisin, Roberto. (2000) CHEST 117, 398S-401S.

5. Connors, AF Jr., Dawson NV., Thomas C, Harrell FE Jr., Desbiens N., Fulkerson WJ., Kussin P., Bellamy P., and Goldman L., Knaus WA. (1996) American Journal of Respiratory and Critical Care Medicine 154, 959-967.

6. Chen, JC., and Mannino, DM. (1999) Current Opinion in Pulmonary Medicine 5, 93-99.

7. Barnes, PJ., and Celli, BR. (2009) European Respiratory Journal 33, 1165-1185.

8. Ekberg-Aronsson, M., Pehrsson, K., Nilsson, JA., Nilsson PM., and Lofdahl, CG. (2005) Respiratory research 6, 98.

9. Brody, JS., and Avrum Spira. (2006) Proceedings of the American Thoracic Society 3, 535-537.

10. Barnes, PJ. (2000). Chest Journal 117, 10S-14S.

11. Khorasani, N., Baker J., Johnson M., Chung KF., and Bhavsar PK. (2015) International journal of chronic obstructive pulmonary disease 10, 283.

12. Forey, BA., Thornton AJ., and Lee PN. (2011) BMC pulmonary medicine 11, 36.

13. Harris, HW. (1963) American Journal of Public Health and the Nations Health 53, 7-15.

14. Cherniack, RM. (1956) Journal of Clinical Investigation 35, 394.

15. Fry, DL., Ebert RV., Stead, WW., and Brown, CC. (1954) The American journal of medicine 16, 80-97.

16. Shapiro, SD., Goldstein NM., Houghton AM., Kobayashi DK., Kelley D., and Belaaouaj, A. (2003) The American journal of pathology 163, 2329-2335.

17. Ogushi, F., Hubbard RC., Vogelmeier C., Fells, GA., and Crystal RG. (1991) Journal of Clinical Investigation 87, 1060.

18. Demedts, I. K., Demoor, T., Bracke, K. R., Joos, G. F., and Brusselle, G. G. (2006) Respir Res 7, 53

19. Leist, Marcel., Single, B., Castoldi AF., Kuhnle S., and Nicotera, P. (1997) The Journal of experimental medicine 185, 1481-1486.

20. Kresch, MJ., Christian, C., Wu, F., and Hussain, N. (1998) Pediatric Research 43, 426-431.

21. Hall, PA., Coates, PJ., Ansari, B., and Hopwood, D. (1994) Journal of Cell Science 107, 3569-3577.

22. Thompson, CB. (1995) Science 267, 1456-1462.

23. Keane, J., Remold, HG., and kornfeld, H. (2000) The Journal of Immunology 164, 2016-2020.

24. Evan, GI., and Vousden, KH. (2001) Nature 411, 342-348.

25. Mercer, J., Mahmoudi, M., and Bennett, M. (2007) Mutation Research/Fundamental and Molecular Mechanisms of Mutagenesis 621, 75-86.

26. Hanahan, D., and Weinberg, RA. (2011) Cell 144, 646-674.

27. Kaufmann, SH., and Earnshaw, WC. (2000) Experimental Cell Research 256, 42-49.

28. Kaina, B. (2003) Biochemical pharmacology 66, 1547-1554.

29. Elmore, S. (2007) Toxicologic pathology 35, 495-516.

30. Kerr, JF., Winterford, CM., and Harmon, BV. (1994) Cancer 73, 2013-2026.

31. Fulda, S., and Debatin, KM. (2006) Oncogene 25, 4798-4811.

32. Dlugosz, PJ., Billen LP., Annis, MG., Zhu, Wijja., Zhang, Z., Lin J., Leber, B., and Andrews, DW. (2006) The EMBO journal 25, 2287-2296.

33. Li, P., Nijhawan, D., Budihardjo, I., Srinivasula, SM., Ahmad, M., Alnemri, ES., and Wang, X. (1997) Cell 91, 479-489.

34. Wajant, H. (2002) Science 296, 1635-1636.

35. Vermeulen, K., Van Bockstaele, DR., and Berneman, ZN. (2005) Annals of Hematology 84, 627-639.

36. Ravichandran, KS., and Lorenz, U. (2007) Nature Reviews Immunology 7, 964-974.

37. Chandra, Joy., Samali, A., and Orrenius, S. (2000) Free Radical Biology and Medicine 29, 323-333.

38. Yee, C., Yang, W., and Hekimi, S. (2014) Cell 157, 897-909.

39. Lee, YH., Cheng, FY., Chiu, HW., Tsai, JC., Fang, CY., Chen, CW., and Wang, YJ., (2014) Biomaterials 35, 4706-4715.

40. Davies, KJ. (2000) IUBMB life 50, 279-289.

41. Carnevali, S., Petruzzelli, S., Longoni, B., Vanacore, R., Barale, R., Cipollini, M., Scatena, F., Paggiaro, P., Celi, A., and Giuntini, C (2003) American Journal of Physiology-Lung Cellular and Molecular Physiology 284, 955-963.

42. Tuder, R. M., Wood, K., Taraseviciene, L., Flores, S. C., and Voekel, N. F. (2000) Chest 117, 241S-242S.

43. Rodgman, A., Smith, C. J., and Perfetti, T. A. (2000) Hum Exp Toxicol 19, 573-595.

44. Baglole, C. J., Bushinsky, S. M., Garcia, T. M., Kode, A., Rahman, I., Sime, P. J., and Phipps, R. P. (2006) Am J Physiol Lung Cell Mol Physiol 291, L19-29.

45. Roos, WP., and Kaina, B. (2006) Trends in molecular medicine 12, 440-450.

46. Phipps, RP., Penney, DP., Keng, P., Quill, H., Paxhia, A., Derdak, S., and Felch, ME. (1989) Am J Respir Cell Mol Biol 1, 65-74.

47. Eickelberg, O., Kohler, E., Reichenberger, F., Bertschin, S., Woodtli, T., Erne, P., Perruchoud, AP., and Roth, M. (1999) American Journal of Physiology-Lung Cellular and Molecular Physiology 276, 814-824.

48. Holz, O., Zuhlke, I., Jaksztat, E., Muller, KC., Welker, L., Nakashima, M., Diemel, KD., Branscheid, D., Magnussen, H., and Jorres, RA. (2004) European Respiratory Journal 24, 575-579.

49. Nyunoya, T., Monick, MM., Klingelhutz, A., Yarovinsky, TO., Cagley, JR. and Hunninghake, GW. (2006) American journal of respiratory cell and molecular biology 35, 681-688.

50. Mimae, T., Hagiyama, M., Inoue, T., Yoneshige, A., Kato, T., Okada, M., Murakami, Y., and Ito, A. (2013) Thorax 69, 223-231.

51. Sun, S. C. (2012) Immunol Rev 246, 125-140.

52. Ghosh, S., May, MJ., and Kopp, EB. (1998) Annual Review of Immunology 16, 225-260.

53. Bonizzi, G., Bebien, M., Otero, DC., Johnson-Vroom, KE., Cao, Y., Vu, D., Jegga, AG., Aronow, BJ., Ghosh, G., Rickert, RC., and Karin, M. (2004) The EMBO journal 23, 4202-4210.

54. Tando, T., Ishizaka, A., Watanabe, H., Ito, T., Lida, S., Haraguchi, T., Mizutani, T., Izumi, T., Isobe, T., Akiyama, T., Inoue, JI., and Iba, H. (2010) Journal of Biological Chemistry 285, 21951-21960.

55. Salminen, A., Huuskonen, J., Ojala, J., Kauppinen, A., Kaarniranta, K., Suuronen, T. (2008) Ageing research reviews 7, 83-105.

56. Gilmore, TD. (2006) Oncogene 25, 6680-6684.

57. Vandermark, ER., Deluca, KA., Gardner, CR., Marker, DF., Schreiner, CN., Strickland, DA., Wilton, KM., Mondal, S., and Woodworth, CD. (2012) Virology 42, 53-60.

58. Angileri, F. F., Aguennouz, M., Conti, A., La Torre, D., Cardali, S., Crupi, R., Tomasello, C., Germano, A., Vita, G., and Tomasello, F. (2008) Cancer 112, 2258-2266.

59. Ruben, SM., Klement, JF., Coleman, TA., Maher, M., Chen, CH., and Rosen, CA. (1991) Genes & development 6, 745-760.

60. Marienfeld, R., May, MJ., Berberich, I., Serfling, E., Ghosh, S., and Neumann, M. (2003) Journal of Biological Chemistry 27, 19852-19860.

61. Weih, F., Warr, G., Yang, H., and Bravo, R. (1997) The Journal of Immunology 158, 5211-5218.

62. Zago, M., Rico de Souza, A., Hecht, E., Rousseau, S., Hamid, Q., Eidelman, D. H., and Baglole, C. J. (2014) Toxicol Lett 226, 107-116.

63. McMillan, D. H., Woeller, C. F., Thatcher, T. H., Spinelli, S. L., Maggirwar, S. B., Sime, P. J., and Phipps, R. P. (2013) Am J Physiol Lung Cell Mol Physiol 304, L774-781.

64.. McMillan, D. H., Baglole, C. J., Thatcher, T. H., Maggirwar, S., Sime, P. J., and Phipps, R. P. (2011) Am J Pathol 179, 125-133.

65. Sheridan, J. A., Zago, M., Nair, P., Li, P. Z., Bourbeau, J. T., W.C. , Hamid, Q., Eidelman, D. H., Benedetti, A. L., and Baglole, C. J. (2015) Respir Res In Press.

66. Mineva, N. D., Rothstein, T. L., Meyers, J. A., Lerner, A., and Sonenshein, G. E. (2007) J Biol Chem 282, 17475-17485.

67. Cormier, F., Monjanel, H., Fabre, C., Billot, K., Sapharikas, E., Chereau, F., Bordereaux, D., Molina, T. J., Avet-Loiseau, H., and Baud, V. (2013) PLoS One 8, e59127.

68. Baglole, C. J., Maggirwar, S. B., Gasiewicz, T. A., Thatcher, T. H., Phipps, R. P., and Sime, P. J. (2008) J Biol Chem 283, 28944-28957.

69. Esser, C., and Rannug, A. (2015) Pharmacol Rev 67, 259-279.

70. Thatcher, T. H., Maggirwar, S. B., Baglole, C. J., Lakatos, H. F., Gasiewicz, T. A., Phipps, R. P., and Sime, P. J. (2007) Am J Pathol 170, 855-864.

71. Rico de Souza, A., Zago, M., Pollock, S. J., Sime, P. J., Phipps, R. P., and Baglole, C. J. (2011) J Biol Chem 286, 43214-43228.

72. Rico de Souza, A. R., Zago, M., Eidelman, D. H., Hamid, Q., and Baglole, C. J. (2014) Toxicol Sci 140, 204-223.

73. Zhang, S., Patel, A., Chu, C., Jiang, W., Wang, L., Welty, S. E., Moorthy, B., and Shivanna, B. (2015) Toxicol Appl Pharmacology.

74. Petrulis, JR., and Perdew, GH. (2002) Chemico-biological interactions 141, 25-40.

75. Evans, BR., Karchner, SI., Allan, LL., Pollenz, RS., Tanguay, RL., Jenny, MJ., Sherr, DH., and Hahn, ME. (2008) Molecular pharmacology 73, 387-398.

76. Vogel, C. F., Sciullo, E., Li, W., Wong, P., Lazennec, G., and Matsumura, F. (2007) Mol Endocrinology 21, 2941-2955.

77. Vogel, C. F., Khan, E. M., Leung, P. S., Gershwin, M. E., Chang, W. L., Wu, D., Haarmann-Stemmann, T., Hoffmann, A., and Denison, M. S. (2014) J Biol Chem 289, 1866-1875.

78. Baglole, C. J., Reddy, S. Y., Pollock, S. J., Feldon, S. E., Sime, P. J., Smith, T. J., and , R. P. (2005) Methods Mol Med 117, 115-127.

79. Carp, H., and Janoff, A. (1978) Am Rev Respir Dis 118, 617-621.

80. Zhivotosky, B., and Orrenius, S. (2001) Curr Protoc Cell Biol Chapter 18, Unit 18 13.

81. Peraza, M. A., Cromey, D. W., Carolus, B., Carter, D. E., and Gandolfi, A. J. (2006) J Appl Toxicol 26, 356-367.

82. Hecht, E., Zago, M., Sarill, M., Rico de Souza, A., Gomez, A., Matthews, J., Hamid, Q., Eidelman, D. H., and Baglole, C. J. (2014) Toxicol Appl Pharmacology 280, 511-525.

83. Oliver, F. J., de la Rubia, G., Rolli, V., Ruiz-Ruiz, M. C., de Murcia, G., and Murcia, J. M. (1998) J Biol Chem 273, 33533-33539.

84. Nicholson, D. W., Ali, A., Thornberry, N. A., Vaillancourt, J. P., Ding, C. K., Gallant, M., Gareau, Y., Griffin, P. R., Labelle, M., Lazebnik, Y. A., and et al. (1995) Nature 376, 37-43.

85. Kroemer, G., Galluzzi, L., and Brenner, C. (2007) Physiol Rev 87, 99-163.

86. Pendergrass, W., Wolf, N., and Poot, M. (2004) Cytometry A 61, 162-169.

87. Leist, M., and Jaattela, M. (2001) Nat Rev Mol Cell Biol 2, 589-598.

88. Xu, Y., Fang, F., St Clair, D. K., Josson, S., Sompol, P., Spasojevic, I., and St Clair, W. H. (2007) Mol Cancer Ther 6, 2048-2056.

89. Zago, M., Sheridan, J. A., Nair, P., Rico de Souza, A., Gallouzi, I. E., Rousseau, S., Di Marco, S., Hamid, Q., Eidelman, D. H., and Baglole, C. J. (2013) PLoS One 8, e74953.

90. Hockley, S. L., Arlt, V. M., Brewer, D., Te Poele, R., Workman, P., Giddings, I., and Phillips, D. H. (2007) Chem Res Toxicol 20, 1797-1810.

91. Caramori, G., Casolari, P., Cavallesco, G. N., Giuffre, S., Adcock, I., and Papi, A. (2011) Int J Biochem Cell Biol 43, 1030-1044.

92. Josson, S., Xu, Y., Fang, F., Dhar, S. K., St Clair, D. K., and St Clair, W. H. (2006) Oncogene 25, 1554-1559.

93. Neumann, M., Klar, S., Wilisch-Neumann, A., Hollenbach, E., Kavuri, S., Leverkus, M., Kandolf, R., Brunner-Weinzierl, M. C., and Klingel, K. (2011) Oncogene 30, 2485-2492.

94. Hailfinger, S., Nogai, H., Pelzer, C., Jaworski, M., Cabalzar, K., Charton, J. E., Guzzardi, M., Decaillet, C., Grau, M., Dorken, B., Lenz, P., Lenz, G., and Thome, M. (2011) Proc Natl Acad Sci U S A 108, 14596-14601.

95. Stringer, K. A., Tobias, M., O'Neill, H. C., and Franklin, C. C. (2007) Am J Physiol Lung Cell Mol Physiol 292, L1572-1579.

96. Mannino, DM. (2002) CHEST Journal 121, 121-126.

97. Yeager, RL., Reisman, SA., Aleksunes, LM., Klassen, CD. (2009) Toxicological Sciences, 111, 238-246.

98. He, Z. H., Chen, P., Chen, Y., He, S. D., Ye, J. R., Zhang, H. L., and Cao, J. (2015) Tob Induc Dis 13, 6.

99. Labonte, L., Coulombe, P., Zago, M., Bourbeau, J., and Baglole, C. J. (2014) PLoS One 9, e112965.

100. Bren, Gary D., Solan, NJ., Miyoshi, H., Pennington, KN., Pobst, LJ., and Paya, CV. (2001) Oncogene 20, 7722-7733.

101. Sasaki, CY., Ghosh, P., and Longo, DL. (2011) Journal of Biological Chemistry 286, 1093-1102.

102. Zago, M., Rico de Souza, A., Hecht, E., Rousseau, S., Hamid, Q., Eidelman, DH., and Baglole, CJ. (2014) Toxicology letters 226, 107-116.